Characterization of Aerosol Emissions from CO_2 Capture Plants treating various Power Plant and Industrial Flue Gases

Hammad Majeed[a] Hallvard F. Svendsen[a]*

[a] *Norwegian University of Science and Technology, Trondheim 7491, Norway*

First Author:

Hammad Majeed
Norwegian University of Science and Technology
E-mail address: hammad.majeed@ntnu.no

Second and Corresponding Author:

*Hallvard F. Svendsen
Norwegian University of Science and Technology
E-mail address: hallvard.svendsen@chemeng.ntnu.no
Corresponding author. Tel.: +47-95141784

Characterization of Aerosol Emissions from CO_2 Capture Plants treating various Power Plant and Industrial Flue Gases

Hammad Majeed[a] Hallvard F. Svendsen[a]*

[a]*Norwegian University of Science and Technology, Trondheim 7491, Norway*

Abstract:

Undesired aerosol formation in gas–liquid contact devices has been a well-known phenomenon in the chemical industry for several decades and can cause severe problems in industrial gas cleaning processes. Several studies indicate that aerosols can govern the total amine emissions from amine based CO_2 capture (PCCC) plants. Despite the importance of aerosol formation and mitigation for the design of a PCCC plant, very little knowledge is available on the characterization and growth of these aerosols.

Four different atmospheric flue gases were modelled in this work, ranging from 4-20% in CO_2 content and representing natural gas, oil and coal fired power plants, and gas from the cement industry. Inlet droplets of size 0.15µ were tested in number concentrations from 1 – 10^7 droplets/cm^3. For 20% CO_2, the effect of intercooling was studied.

The findings are:

Aerosol droplets grow from their initial size regardless of their initial composition and type of flue gas processed. The initial composition of the droplets has a significant effect on emissions.

With increasing CO_2 concentration, more carbamate is formed relative to free MEA. This leads to less effective water wash and significantly higher final emissions.

With low droplet number concentration no visible depletion of MEA in the absorber and water wash sections was found for any of the CO_2 concentrations. At 10^7 droplets/cm^3, gas phase MEA partial pressure changes are clearly seen, first in the water wash, and then, at higher contents, the effect starts lower and lower down in the absorber.

The carry-over of amine into the water wash increases with increasing gas phase CO_2 content. However, the effect on the gas phase MEA content in the water wash goes through a maximum caused by strong carbamate formation at high CO_2 concentrations.

The droplet temperature profiles are unaffected by number concentration and initial composition of aerosol droplets.

It is found that the water wash section reduces significantly the aerosol-based, and thereby the total, amine emissions. The effect of the water wash is reduced when the flue gas CO_2 content increases.

Intercooling lowers the partial pressure of MEA in both absorber and water wash significantly. This reduces the droplet growth and MEA content. The combined effect is a strong reduction in MEA emissions; in the case of 20% CO_2 in the flue gas, by a factor of 5-10.

Keywords:

Aerosol growth, Amine emission, Absorption columns, Post-combustion CO_2 capture, Flue gas CO_2 content, Internal droplet profiles

Introduction:

Worldwide energy consumption is increasing on an average of 2% yearly. In order to meet these demands, energy production from fossil fuels will remain important for decades to come. The contribution from renewable energies is expected to grow steadily as well but still, fossil energies will be important. Energy from nuclear sources is predicted to grow only moderately (IEA, 2016).

The most significant global challenge today and in the forthcoming years is to reduce the global CO_2 emissions, as this is one of the key drivers of global climate change. Carbon dioxide capture, transport and storage has gained increased interest as an intermediate solution towards a sustainable energy system in the long run (IPCC, 2005). Emission reduction targets of 80–90% of CO_2 from emission sources are usually conferred in the context of targets that can be attained by CCS technologies (MacDowell et al., 2010).

CO_2 is produced in large quantities by fossil fuel-fired power plants, in steel production, cement production, in the production of petrochemicals and in natural gas purification. Carbon dioxide capture by absorption processes is one of the most mature industrial technologies to date for CO_2 emissions mitigation. 30wt% aqueous Monoethanolamine (MEA) solution can be considered as a base case solvent for a typical PCCC plants (Abu-Zahra, 2009; Rochelle, 2009). The CO_2 content in flue gases varies depending upon the source. Flue gas from coal-fired power plants typically contains around 12-14% CO_2 while those from a natural gas turbine are at around 3-4%, (Global CCS Institute, 2013).

Cement plant flue gas has normally higher flue gas CO_2 content, typically around 20-25%, whereas in steel plants the flue gas CO_2 content may be even higher. Amine-based PCCC plants developed for CO_2 capture from coal or natural gas-fired power plants have been shown also to be suitable for use in cement plants (IEAGHG, 2008). Aker solutions operated its mobile test unit at Norcem cement plant in Brevik and successfully tested the technology (Knudsen et al., 2014)

Studies show that amine based PCCC plants have amine emissions to the air, while possibly also forming other compounds in the atmosphere (Knudsen and Randall, 2009). Amines are volatile and will be emitted via the exiting gas. The formation of aerosol in gas-liquid contact devices has, in some cases, been found to be a major contributor to these emissions (IEAGHG, 2010; Mertens et al., 2012).

The issue of aerosol based emissions has only been reported recently so little information is available in this area. There are studies that deal with the prediction and measurement of amine emission based on aerosols as well as demonstrating emissions reduction methods. Most of these studies are experimental investigations that do not deal with the inner characterization of droplets. For details see (Fulk, 2016; Khakharia et al., 2014a; Mertens et al., 2012; Moser et al., 2014; Saha and Irvin, 2017). Some current studies, however, show modelling results for aerosol droplets in absorption columns (Kang et al., 2017; Zhang et al., 2017).

Scope of work:

In order to understand the mechanism of aerosol formation and growth, numerical models are required that can predict the development of droplet composition and size as function of operational and solvent characteristics. This can provide an improved understanding of the governing processes and help in designing appropriate countermeasures to reduce the total emissions. A basic simulation tool for the description of single and multiple aerosol droplets behaviour in CO_2 absorption columns is already established and described in (Majeed et al., 2017b, 2017a).

The main theme of the current work is to investigate how aerosol droplet growth, composition change, and resulting emissions, vary with the source of CO_2. It will thereby provide an aid in designing mitigation units, like setting targets for cut size or separation efficiency in demisting equipment.

The work covers a broad range of emissions exemplifying most of the large CO_2 emitting sources. Although CO_2 and water content along with temperature for a given emission source varies over time, in order to simplify the model work, one single concentration of CO_2 will be used for each case.

For each flue gas case, a separate simulation is performed in CO2SIM(Luo et al., 2009; Tobiesen et al., 2012, 2007). The selected gas sources are presented in Table 1. Flue gases from combustion of respectively natural gas, fuel oil and coal and of gases from the cement industry were chosen. The volumetric CO_2 contents were set to 4%, 8%, 12% and 20% respectively, in the flue at the inlet of the absorber.

The inlet gas is assumed to pass through a direct contact cooler making the gas temperature the same in all cases, thus also the water content will be the same at the inlet of the absorber. In addition, we have simulated a cement flue gas case where intercooling is applied in the absorber.

An absorber column of 15 m is used equipped with two water washes of 2m each. 30 wt% MEA solution with a lean loading of 0.25 is used as solvent and the absorption rate is kept at 90% in all cases. The remaining parameters, e.g. column and water wash diameters, flow rates etc. are adjusted in every case in such a way that they meet the requirement of 90% CO_2 absorption.

Table 1: Exhaust flue gas composition from different point sources

	Natural Gas / Flue Gas 1	Fuel Oil / Flue Gas 2	Coal / Flue Gas 3	Cement industry / Flue Gas 4
CO_2 %	4	8	12	20
Water %	8.5	8.5	8.5	8.5
Inert %	87.5	83.5	79.5	71.5
Temperature (K)	327	327	327	327
Pressure (kPa)	109	109	109	109

Modelling:

The work started with flow sheet simulations in CO2SIM. This is a flexible tool for solving and modelling advanced chemical processes related to carbon capture technologies. It has relatively stable numerics which allows simulation of advanced process configurations for process optimization (Einbu, 2016). The flow sheet used in the current work is shown in Figure 1. All four cases (Flue gas sources) were simulated without taking into account the aerosol phase. The simulations result in gas and liquid phase composition and temperature profiles along the column. Only the liquid phase profiles were used in the further modelling, considering that the liquid phase composition and temperature may not be affected by the aerosol phase. The gas phase profiles were calculated inside the aerosol model, taking into account both heat and mass transfer between the gas phase and bulk liquid and between the gas phase and the aerosol phase. Similarly, the aerosol droplet internal profiles were calculated by differential balance equations for heat and mass. These equations are coupled with a reaction rate model, vapor-liquid and chemical equilibrium model as well as models for heat and mass transfer between gas and aerosol phase and between gas and bulk liquid phase. For a detailed explanation of model and basic assumptions, see (Majeed et al., 2017b, 2017a).

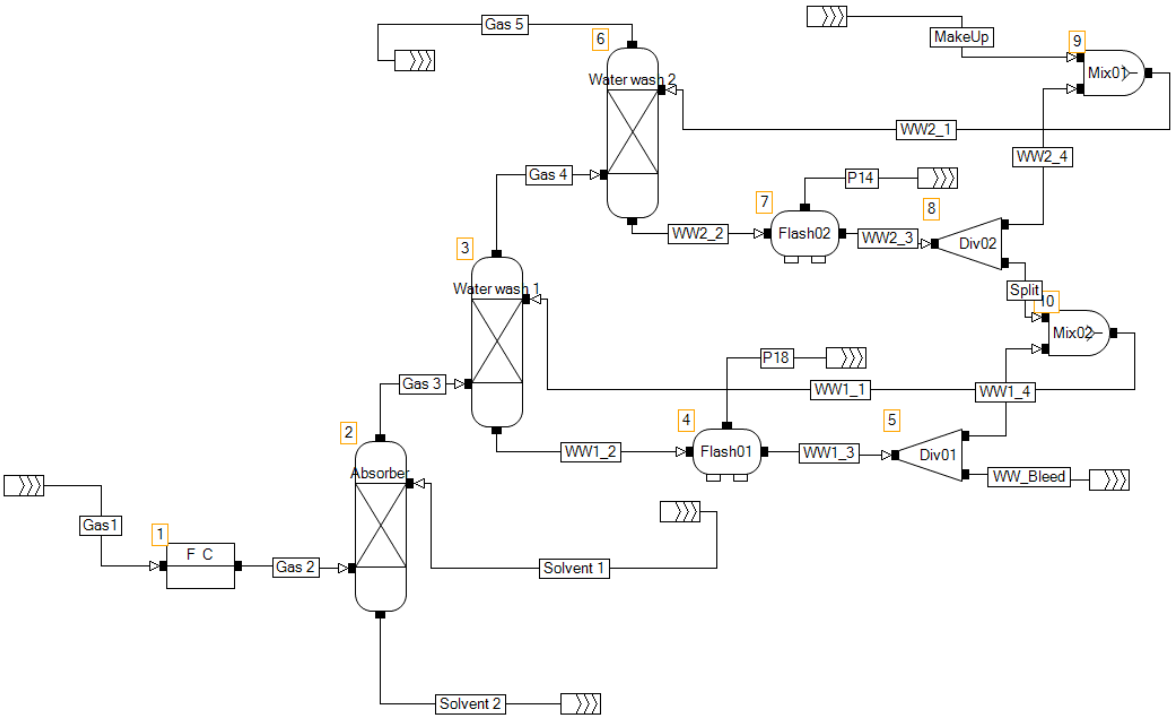

Figure 1: Flowsheet for absorber and water wash for PCCC plant from CO2SIM. For abbreviations explanations see Notations table.

Results and Discussions:

The basics of the simulations were described in the previous section and in order to present results for all flue gas sources, two aerosol cases are modelled by specifying different inlet conditions for the aerosol droplets. The liquid phase concentration and temperature profiles from CO2SIM for all flue gas sources are presented in Figure 2, and, as mentioned earlier, are used as basis for the further modelling. It is seen that the main differences between the cases are the temperature and total CO_2 concentration profiles. With increasing CO_2 content in the inlet gas, the temperature in the absorber section increases significantly. This will increase the amine volatility and thereby possibly affect the growth of the aerosol droplets. On the other hand, an increased gas phase CO_2 content will increase the CO_2 loading of the liquid phase as seen by the increased total CO_2 concentration. This will lower the free amine concentration and thereby reduce the amine volatility. Thus, the two effects counteract each other.

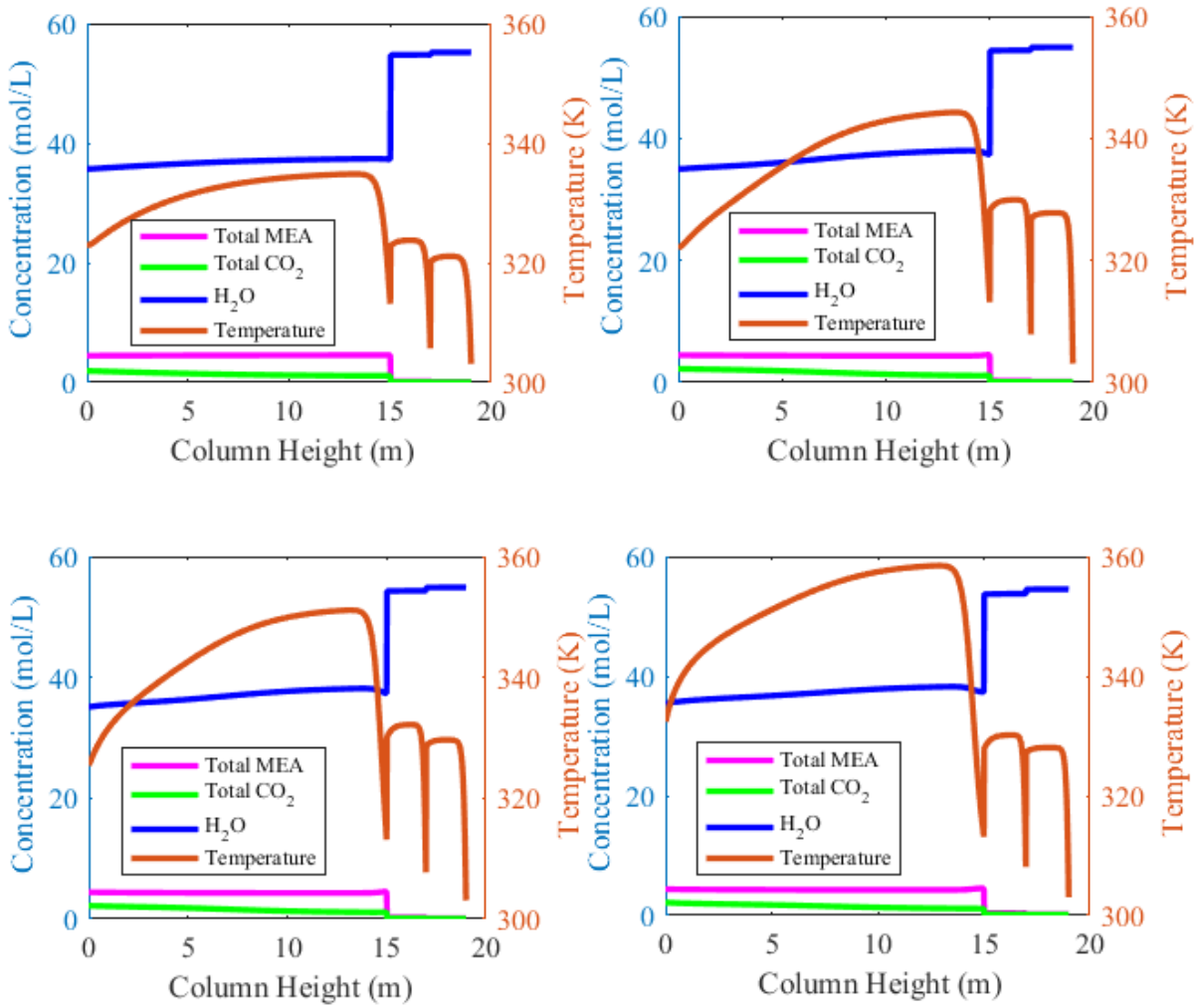

Figure 2: Liquid phase profiles throughout the column, Top row: (a) Flue gas 1, (b) Flue gas 2, Bottom row: (c) Flue gas 3, (d) Flue gas 4

For detailed information about implementation of the CO2SIM model see (Majeed and Svendsen, 2017). Two different scenarios are shown in Table 2, and adopted for all four flue gas types. One, in which the inlet droplets contain 5M MEA, while in the other case the droplets enter with the flue gas as pure water droplets. The pure water droplets is an analogue to inert particles entering the absorber, on which water can start to condense by heterogeneous nucleation. The droplets have a velocity relative to the gas phase equal to the terminal velocity, which in all cases is very low. The initial size of the droplets is the same in all the cases and taken as 0.15µm. This is the typical size range reported in various literature (Khakharia et al., 2015, 2014b). The aerosol droplets will undergo changes in terms of internal composition and temperature as well as growth. From the absorber section, the droplets enter straight into water wash 1 where the water is circulated at a specific rate. Subsequently they enter into water wash 2, operating in a similar way, and then leave the water washes with the treated flue gas. For all cases, droplet number concentrations ranging from $1 - 10^7$ droplets/cm^3 are modelled.

Table 2: Modelled Cases

Case 1	Droplet initial radius 0.15μm, containing 0.0001M MEA travelling from bottom to top of column (0-19m) for all flue gas sources i.e. 1,2,3 and 4, by varying droplet number concentration, c_N= 1-10^7 droplets/cm^3
Case 2	Droplet initial radius 0.15μm, containing 5M MEA travelling from bottom to top of column (0-19m) for all flue gas sources i.e. 1,2,3 and 4, by varying droplet number concentration, c_N= 1-10^7 droplets/cm^3

In the following, we present results first for Case 1, for 10^3 and 10^7 droplets/cm^3. Results for single droplet are only shown for growth. The droplet internal profiles for 1 drop are practically identical to 10^3 droplets/cm^3. In order to save space, concentration and temperature profile results for 10^5 droplets/cm^3 are only given in supplementary information and discussed in the text together with the other number concentrations.

Case 1:

In case 1, droplets with an initial radius of 0.15μm containing 0.0001M MEA enter with the 4 different gas phases. They are, in the absorber and water wash, exposed to the bulk liquid profiles as shown in Figure 2. It is, as already mentioned, assumed that the bulk liquid profiles remain unaffected by the aerosol phase for all droplet number concentrations. The predicted droplet internal free MEA profiles as function of position in the absorber and water wash for all flue gas sources are shown in Figure 3. Similarly in Figures 4 and 5, the free CO_2 and carbamate concentration profiles are shown. In Figures 6-8 respectively, the gas phase MEA profiles, droplet internal temperature profiles and droplet growth curves are shown.

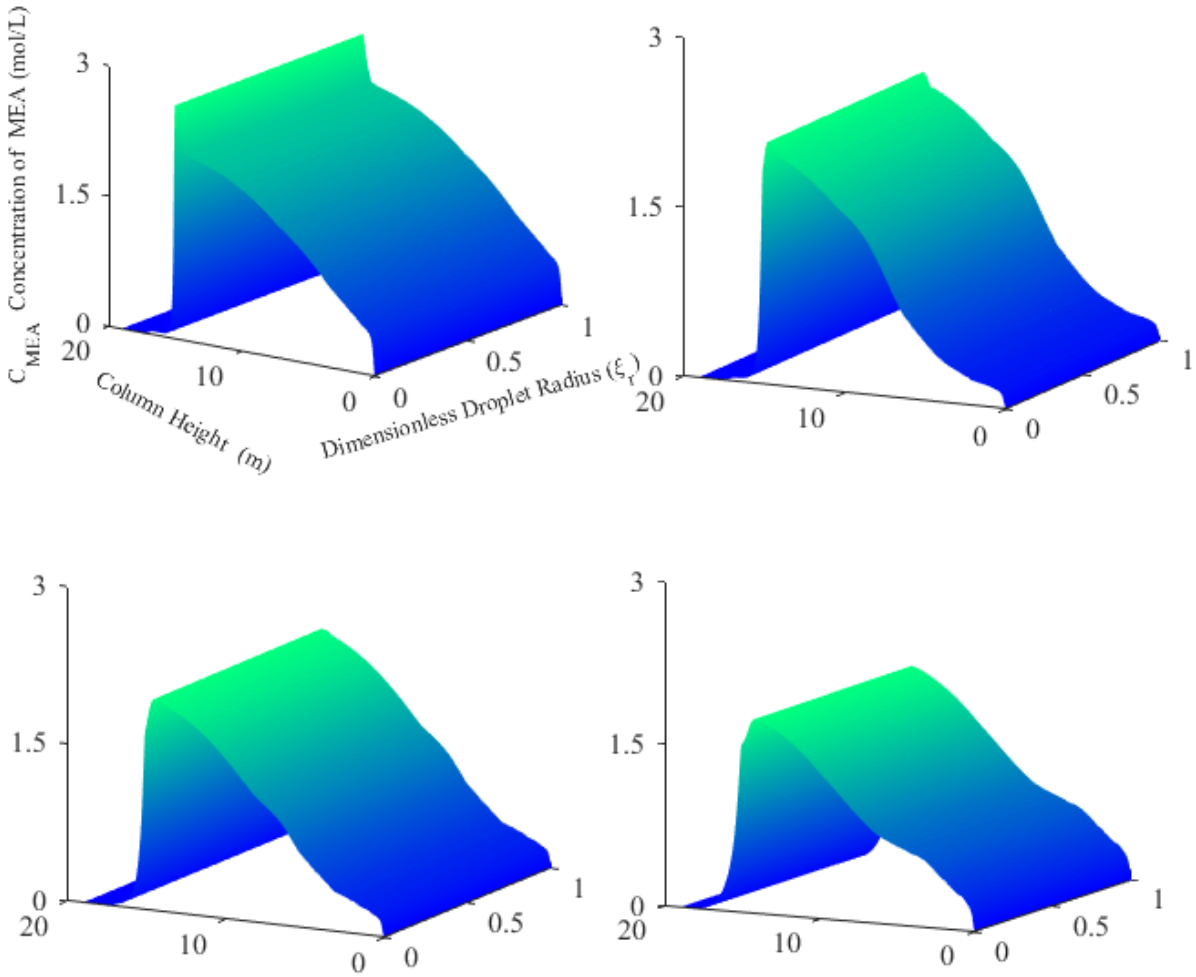

Figure 3: Free MEA concentration profiles as function of position for $c_N = 10^3$ droplets/cm^3
Top row: (a) Flue gas 1, (b) Flue gas 2, Bottom row: (c) Flue gas 3 (d) Flue gas 4

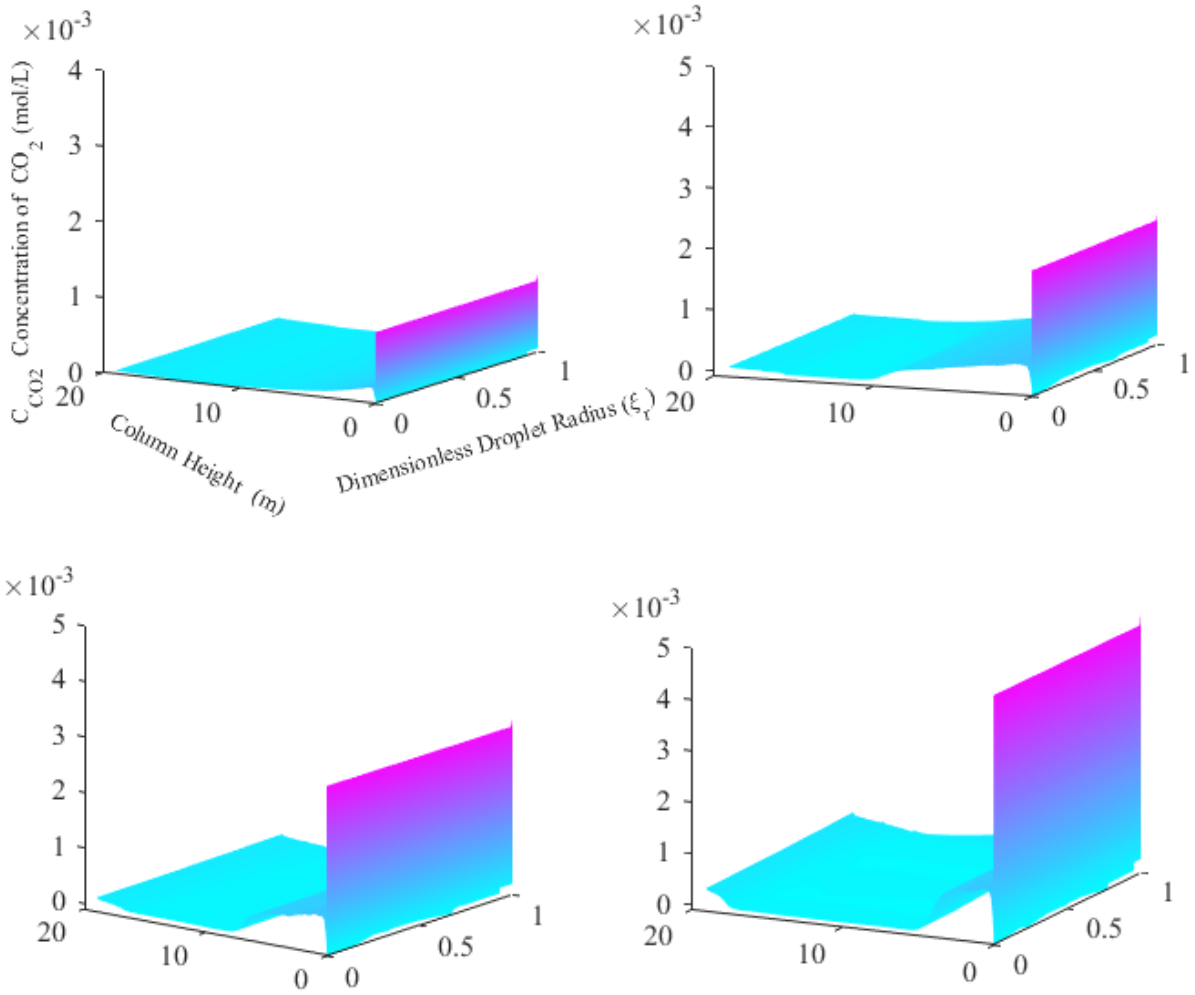

Figure 4: CO_2 concentration profiles as function of position for $c_N = 10^3$ droplets/cm^3

Top row: (a) Flue gas 1, (b) Flue gas 2, Bottom row: (c) Flue gas 3 (d) Flue gas 4

Figure 3a shows MEA profiles for flue gas 1. In this case the bulk liquid phase CO_2 loadings in the absorber are the lowest, but so are also the temperatures. Initially the free MEA concentration increases rapidly, and then continues to increase more slowly throughout most of the absorber, and finally a more rapid increase toward the absorber top is seen. The main reason for the fast increase in free MEA concentration at the bottom of the column is rapid evaporation of water leading to a concentrating up of MEA. Simultaneously, CO_2 is rapidly absorbed and carbamate is formed, as can be seen in Figures 4a and 5a respectively. The CO_2 profiles illustrate the very rapid build-up of CO_2 concentration followed by a rapid reduction in concentration caused by carbamate formation. Then, as carbamate builds up, the free CO_2 concentration increases again. Further up in the absorber, because of lower gas phase CO_2 pressure, there is a reversion of carbamate giving more free MEA and at the same time a desorption of CO_2 and less free CO_2 in the droplet. Going up in the absorber column, the gas phase MEA pressure increases, see Figure 6, partly because of increased temperature, see Figure 7a, but also because of reduced bulk liquid CO_2 loading, see Figure 2. This gives a positive driving force for MEA into the droplets, and at the same time water starts transferring to the droplets. At about 7-8m into the absorber column, we see that this leads to an increase in droplet size, see Figure 8.

At the very top of the absorber, the temperature falls because of lean amine solution entering at 40 ^{0}C. This fall in temperature leads to increased absorption of CO_2 caused by a shift in equilibrium and increased transfer of MEA and water to the droplets. The combined effect is a more rapid increase in droplet size, as seen for the last half meter form the absorber top (at 15m).

When the droplets enter the first water wash, MEA starts desorbing rapidly out of droplet. At the same time water condenses on the droplet surface because of the temperature reduction. This increases both droplet volume and temperature. The processes taking place in the second water wash are similar. As seen in Figure 8a, more than 80% of the droplet growth takes place in the water wash sections and the initially 0.15µ radius droplets increase in size to about 2.7 µ in radius for the case of 1000 droplets/cm^3.

A similar behaviour is observed when flue gases from other fuel sources (oil, coal, cement) are fed to the absorption column. The profiles for free MEA, free CO_2, carbamate concentrations and temperature are shown in the b, c and d parts of Figures 3, 4, 5 and 7.

Comparing the a and b parts of Figures 3 and 5 (flue gas 1 and 2) it is seen that higher driving forces for CO_2 allows more transfer of CO_2. The carbamate formation initially increases more rapidly for flue gas 2 and subsequently the increase in free MEA inside the droplet is reduced for flue gas 2 compared to flue gas 1. The reduced concentration of free MEA in the case of flue gas 2 is maintained throughout the absorber and the carbamate levels are higher. This is reasonable as the droplet concentration levels will follow the bulk liquid concentration levels to a large extent. These trends are also reflected in the free CO_2 concentration which is seen initially to increase rapidly and then fall to levels higher than for flue gas 1. When the droplets enter the water wash section, both the droplet free MEA and carbamate concentrations go down, but remain higher than for flue gas 1. These findings are reasonable as more MEA is passed from the absorber to the water washes, thus increasing the total MEA level also in the wash water. At the exit of the second water wash the droplets still contain 0.0065 mol/L of MEA and 0.035mol/L of carbamate. In Figure 6 the gas phase MEA profiles for flue gas type 2 are given. We see that up to about 7m into the absorber, the MEA partial pressure remains lower for flue gas 2 compared to flue gas 1. The reason for this is the combined effect of increased carbamate formation, resulting in a lower fraction of free MEA, and an increased droplet temperature because of the heat of reaction. The temperatures are shown in Figure 7b and we see that initially the temperature with flue gas 2 increases a few degrees more than with flue gas 1. However, this temperature increase, and the resulting equilibrium shift, is not enough to counter the increased carbamate formation and subsequent free MEA concentration decrease. Combined, this explains the reduction in MEA partial pressure seen up to about 7 m in Figure 6.

Moving further up in the absorber section, the difference in temperature between flue gas 1 and 2 increases. Now the temperature effect becomes the strongest, leading to higher MEA partial pressures for flue gas 2.

Droplet growth is shown in Figure 8. Comparing 8a and 8b it is clearly seen that the droplet growth is much stronger with flue gas 2. For flue gas 2, the final droplet size is about 5.5µ compared to 2.7µ for flue gas 1. This is reasonable as higher gas phase CO_2 levels will shift the equilibrium toward carbamate (and protonated amine) rather than free amine. Thus, maintaining higher driving forces for MEA, in particular in the lower half of the absorber. This results in lower water surface pressure and increased condensation.

We see that also for flue gas 2, the droplets continue to grow in the water wash, but compared to flue gas 1, the growth in the absorber part is much stronger, mainly because of the temperature increase in the upper part giving higher water vapour pressures. Even though no visual depletion of the gas phase is seen with 1000 droplet/cm^3, not shown in Figure 6, this effect is visible in the growth curves, giving slightly less growth with 1000 compared to 1 droplet/cm^3, as seen in Figure 8.

Results when coal based flue gas is fed to the absorption column, i.e. flue gas 3, are presented in Figures 3c,4c,5c. The differences seen between flue gas 1 and flue gas 2 are further accentuated for flue gas 3. The free MEA concentration, see Figure 3c, is lower at the top of the absorber for flue gas 3 compared to flue gas 2, but in the middle part of the column, a small increase is seen in the coal based flue gas case. This is also reflected in Figure 5c where the carbamate formation for flue gas 3 is slightly lower than for flue gas 2. The reason for this is found in the temperature profiles in Figure 7c. For flue gas 3 the temperature bulge starts lower down in the column, but the top point is not so much higher than for flue gas 2. This means that the temperature effect on the equilibrium is more important in the low to middle section of the absorber for flue gas 3. This can also be seen in Figure 6 where the gas phase MEA partial pressures are much higher, relatively speaking, for flue gas 3 compared to flue gas 2. In the water wash sections, the droplets lose most of their MEA and the concentration of MEA and carbamate at the exit from the second water wash in gas phase are found to be 0.0021 and 0.076 mol/L respectively.

Droplet growth is shown in Figure 8c. With flue gas 3, the growth is stronger than with flue gas 2, and the final droplet size is about 8µ. Almost half the growth takes place in the absorber in this case and there is a small difference in growth in the water washes between 1000 compared to 1 droplet/cm^3 indicating that the gas phase MEA partial pressures have changed slightly, although not visible in the gas phase MEA profiles when comparing 1(not shown) and 1000 droplets/cm^3.

The results for the cement industry based flue gas, i.e. flue gas 4, are shown in Figures 3d, 4d and 5d. The profiles exhibit basically the same characteristics as seen previously. The effect of temperature is even stronger than for flue gas 3, leading to higher free MEA concentrations and lower carbamate concentrations in the lower and middle sections of the absorber. At the top, both the free MEA and carbamate concentrations are higher. The strong temperature effect also leads to higher gas phase MEA partial pressures throughout the column as seen in Figure 6.

When droplets enter the water wash sections, the concentrations of free MEA and carbamate go down and reach an outlet level of 0.0005 mol/L and 0.22 mol/L. We see that the total MEA concentration in the droplets at the outlet goes up with increasing CO_2 partial pressure in the inlet gas and that the ratio between free MEA and carbamate goes down. This is reasonable because of increased loading.

From Figure 8d is seen a further droplet growth for this flue gas to about 11 µ. Also the absorber plays a more important role in droplet growth and the difference between 1000 and 1 droplet/cm^3 is larger. Even in this case, with flue gas 4, the gas phase MEA depletion is not visible in the MEA partial pressure curves (not shown). However, a small depletion does take place, leading to the difference in growth curves in Figure 8d.

Comparing the MEA profiles from Figures 3a,b,c and d it is seen that the instant build-up of free MEA concentration at the very bottom of the column gradually decreases as water evaporation becomes less rapid with increasing CO_2 content in the flue gas. This is also reflected in the temperature profiles.

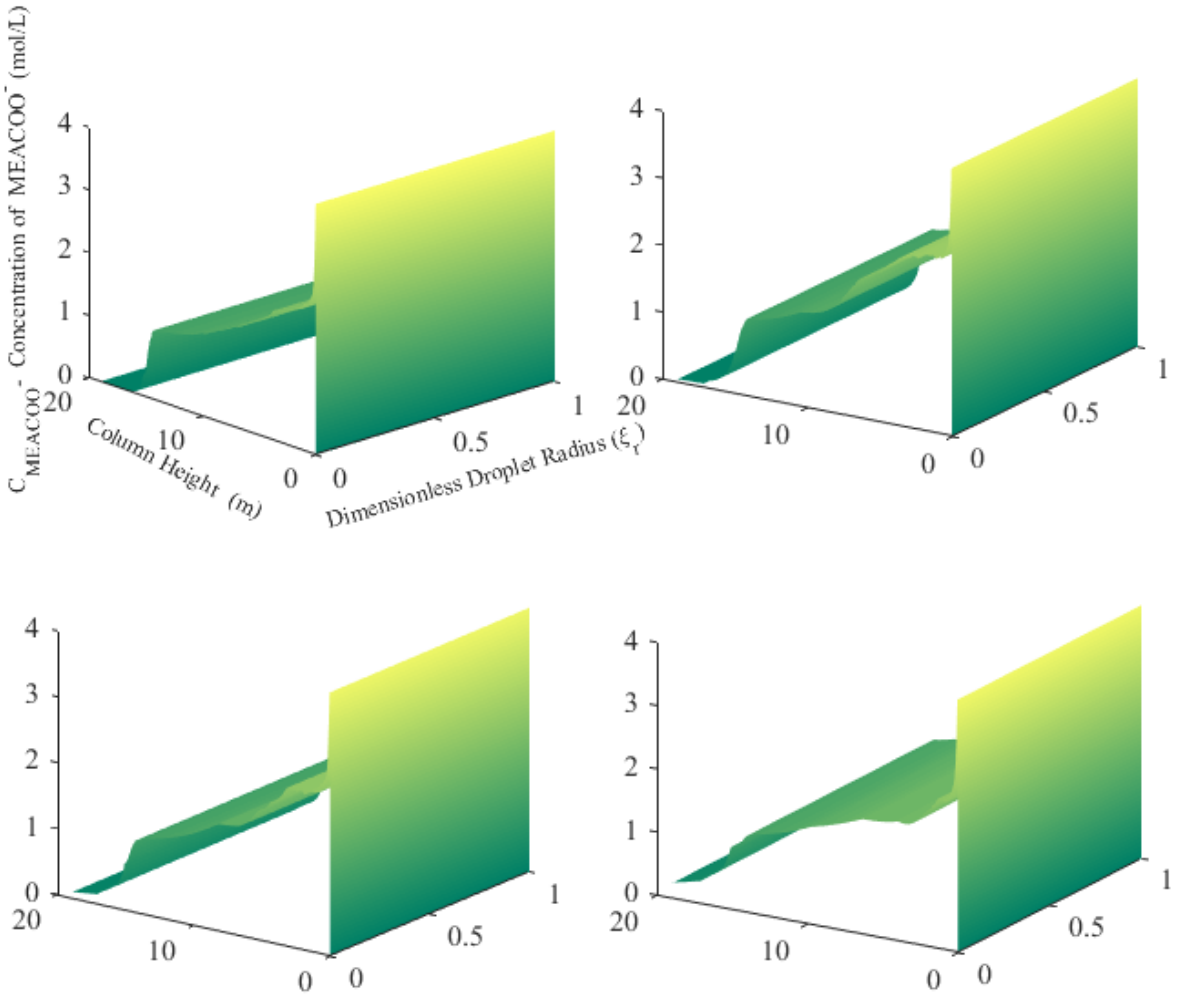

Figure 5: Carbamate concentration profiles as function of position for $c_N = 10^3$ droplets/cm^3
Top row: (a) Flue gas 1, (b) Flue gas 2, Bottom row: (c) Flue gas 3 (d) Flue gas 4.

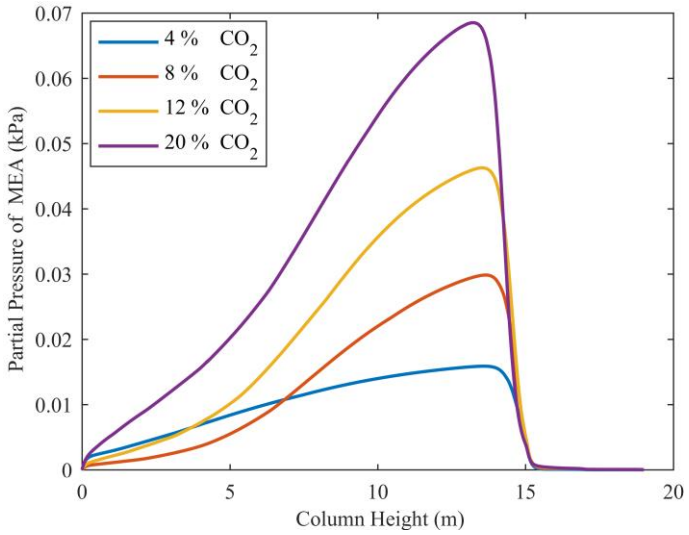

Figure 6: Case 1: Gas phase MEA partial pressure profile for c_N= 10^3 droplets/cm^3

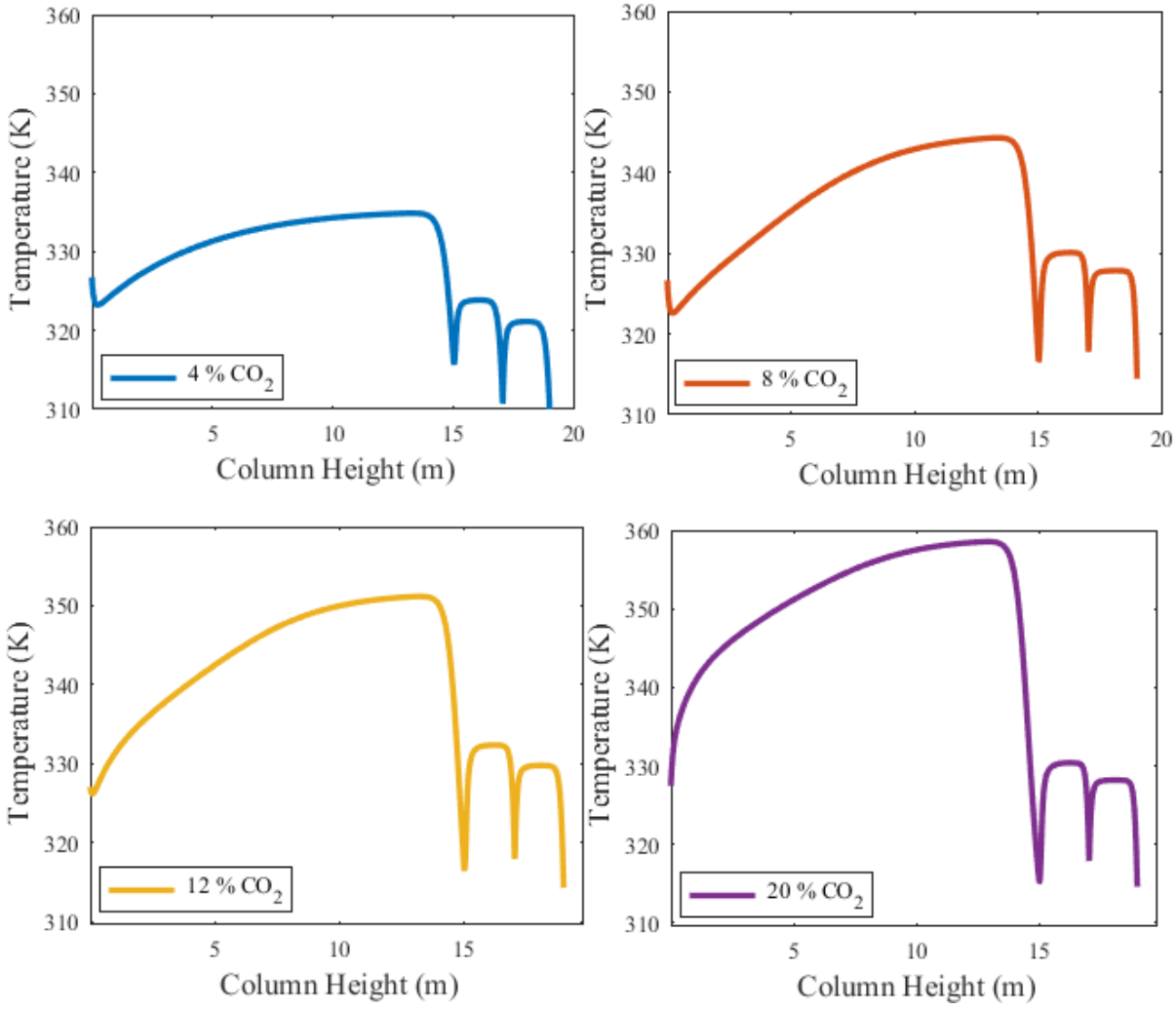

Figure 7: Case 1: Droplet temperature profiles as a function of position for c_N= 10^3 droplets/cm^3, Top row: (a) Flue gas 1, (b) Flue gas 2, Bottom row: (c) Flue gas 3 (d) Flue gas 4.

When comparing the droplet temperature profiles, as given in Figure 7, we see that for flue gas 1 there is a rapid initial temperature decrease. The droplet temperature is affected by water evaporation, MEA and CO_2 absorption and the reaction between CO_2 and MEA. With flue gas 1, the evaporation of water is dominating and leads to a drop in temperature. As the gas phase CO_2 concentration increases, still evaporation takes place, but the exothermic reaction forming carbamate becomes more and more important. With 20% CO_2 as in flue gas 4 we see that the droplet temperature starts rising from the very beginning.

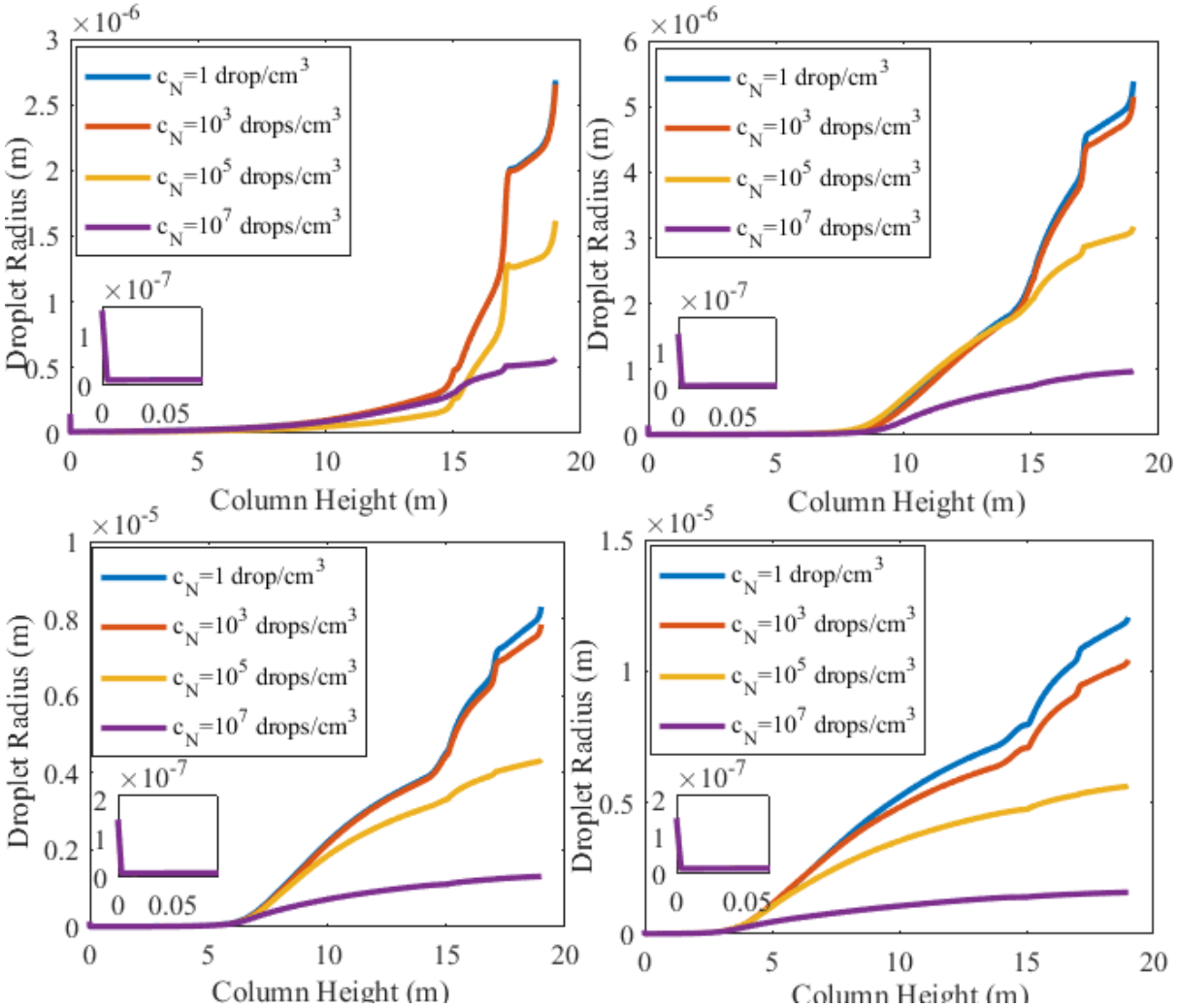

Figure 8: Case 1: Growth of aerosol droplets for all number concentrations, Top row: (a) Flue gas 1, (b) Flue gas 2, Bottom row: (c) Flue gas 3 (d) Flue gas 4.

Increasing the droplet number concentration to 10^5 droplets/cm^3, the free MEA, CO_2 and carbamate profiles are shown in the supplementary information as Figures S1, S2 and S3. There is no change in the temperature profile so this is not included.

From Figure 8 we see that when the droplet number concentration is increased to 10^5 droplets/cm^3, the effect of MEA depletion or carry-over in the gas phase becomes significant. For the two lowest CO_2 concentrations, flue gas 1 and 2, only the growth in the water washes is influenced, whereas for flue gas 3 and 4 the changes in droplet size starts lower down in the absorber. This is more thoroughly discussed later for the highest droplet number concentration.

When increasing the droplet number concentration to 10^7 droplets/cm^3 the effect on gas phase MEA depletion and carbamate build up is strong for most flue gas sources. The droplet internal variable profiles are presented in Figures 9, 10 and 11. The gas phase MEA profiles are shown in Figure 12 indicating depletion of MEA from the gas phase when compared with figure 6, but, as seen, the change in depletion when increasing the droplet number concentration depends on the CO_2 concentration.

Comparing Figures 3a and 9a we see that for flue gas 1(natural gas), there is not a large change in the free MEA profiles. Also for 10^7 droplets/ cm^3 there is a rapid initial increase in free MEA and it continues to rise similar to what seen in Figure 3a, but the rapid increase at the top of the absorber is smaller. Also, the carbamate and free CO_2 profiles shown in Figures 10a and 11a are very similar to those in Figures 4a and 5a. The reason for this is that the gas phase MEA partial pressure profile is not significantly affected by the high droplet number concentration as seen when comparing the curves for Flue gas 1 in Figures 6 and 12. This finally leads to only a small change in droplet growth, as seen in Figure 8a. Only during the last 0.5m of the absorber can we see a significant change in growth.

However, already at a CO_2 concentration of 8% in the flues gas (Flue gas 2), significant changes take place. Comparing Figures 3b and 9b we see that for the first 8m of the absorber, the profiles are quite similar, rising to about 1.4 mole/L of free MEA. After this point, in the low droplet number case, the free MEA concentration continues to rise, whereas for 10^7 droplets/ cm^3 there is a decrease in free MEA. At the same point in Figure 10b we see that the carbamate concentration increases, thus shifting free MEA to carbamate at that point in the column. Further up, the free MEA concentration increases again because of higher temperature, see Figure 13, and thereby higher MEA volatility. In Figure 12 we see that for the first 8m the curve for 8% CO_2 is very close to the one in Figure 6. At this point, however, in Figure 12, a gas phase depletion of MEA is seen. This reduces the droplet up-take of MEA, and thereby also of water. This "shortage" of MEA inside the droplet is the cause of the shift to more carbamate relative to free MEA. The MEA depletion affects the growth of the droplets and in Figure 8b we see that about at 8m into the absorber, the growth curves for the low and high droplet numbers part.

For flue gas 3(Coal) and flue gas 4 (Cement) the changes, compared to the previous case, are similar but stronger. For coal based exhaust, the effect of droplet number concentrations comes at about 6m into the absorber, and for cement based flue gas, the effect appears already after about 3m. This leads to earlier and more gas phase depletion as seen in Figure 12, which again leads to a decrease in free MEA concentration, see Figure 9. As the temperature rise is higher for the higher CO_2 concentrations, the free MEA concentration and gas phase MEA partial pressure both increase when going further up in the absorber, and most for the highest CO_2 concentration.

Moving into the water wash section, we see in the magnified graph in Figure 12, that there is a carry-over of MEA from the absorber to the water wash caused by the droplets. It is interesting to note that the carry-over does not increase with CO_2 concentration for all tested concentrations.

For flue gas 1(Natural Gas), the carry-over is hardly visible. However, for flue gas 2 and 3 (Oil and Coal), the carry-over apparently is at its highest, and then drops when considering flue gas 4 (Cement). The carry-over which appears in the MEA partial pressures in Figure 12 is a function of several mechanisms. It depends on the total MEA concentration in the droplets and

the droplet size. However, it also depends on how fast the MEA can desorb from the droplets once they enter the water wash. As the total MEA concentration in the droplets does not vary dramatically, the droplet size at the absorber outlet and the desorption rate are the main governing variables. The droplet size at the absorber outlet increases with inlet gas CO_2 concentration to respectively 0.3, 0.7, 1.1 and 1.4µ in radius for flue gases (1, 2, 3 and 4) having 4, 8, 12 and 20% CO_2 at the inlet. So basically there is more carry-over to the water wash for the higher CO_2 concentrations. However, since the CO_2 removal rate is limited to 90%, the remaining CO_2 in the gas in the water wash will also increase. This leads to a shift to more carbamate in the droplets and subsequently to lower free MEA concentrations. The lower free MEA concentrations will reduce the desorption rate and thereby the increase in MEA partial pressure in the water wash. Thus desorption from the droplets in the water wash will be reduced by high outlet CO_2 concentrations and they will retain more total MEA.

As the inlet CO_2 concentration increases, more of the droplet growth takes place in the absorber. This is most accentuated for the low droplet number concentrations where the droplet size increases 10-fold in the water wash with 4% CO_2 in the inlet gas (Flue gas 1). With 20% CO_2 in the inlet gas (Flue gas 4) the size increase in the water wash is less than 40%. For 10^7 droplets/ cm^3 the size increase in the water wash is much smaller, ranging from 100% to 10% when going from 4 to 20% CO_2.

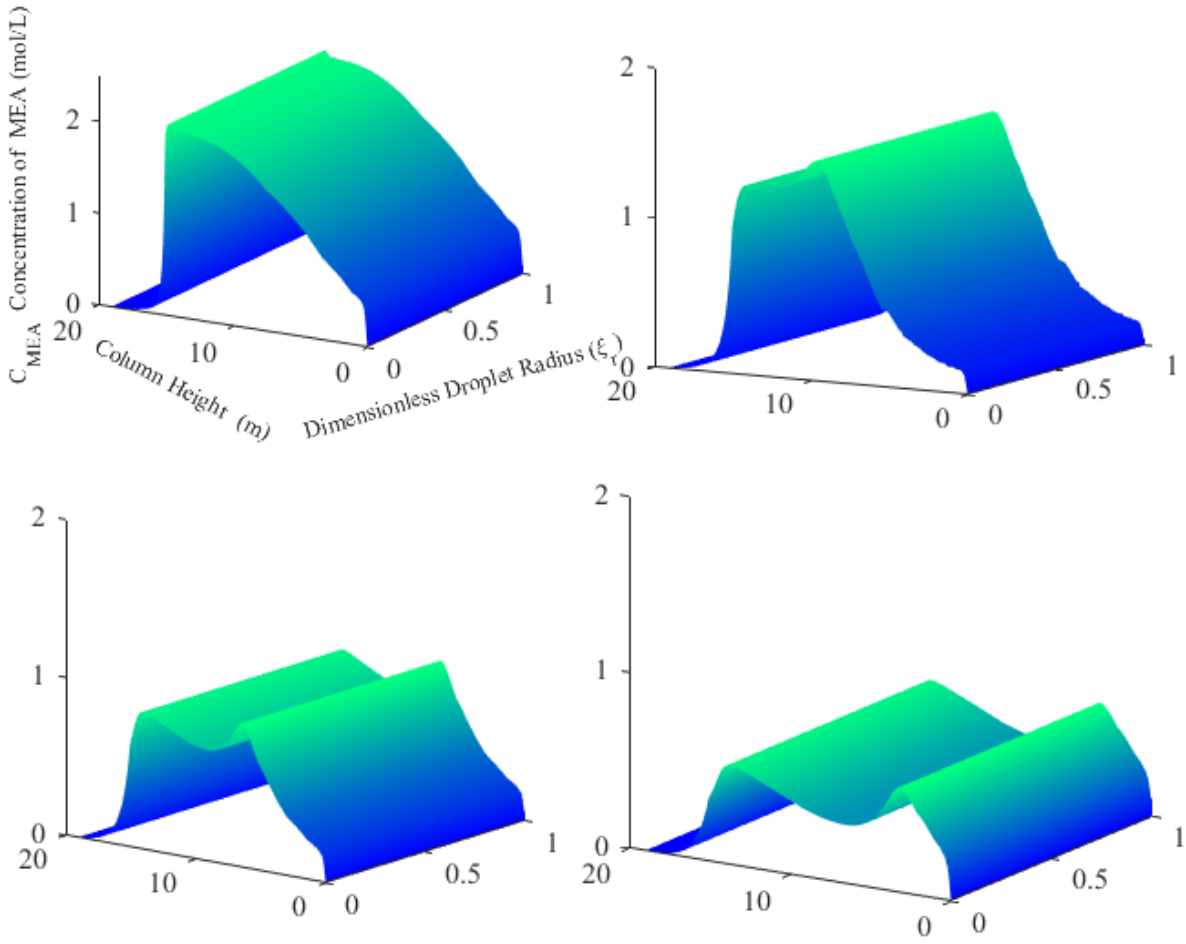

Figure 9:Case 1: Free MEA concentration profiles as a function of position for $c_N = 10^7$ droplets/cm^3,Top row: (a) Flue gas 1, (b) Flue gas 2, Bottom row: (c) Flue gas 3 (d) Flue gas 4

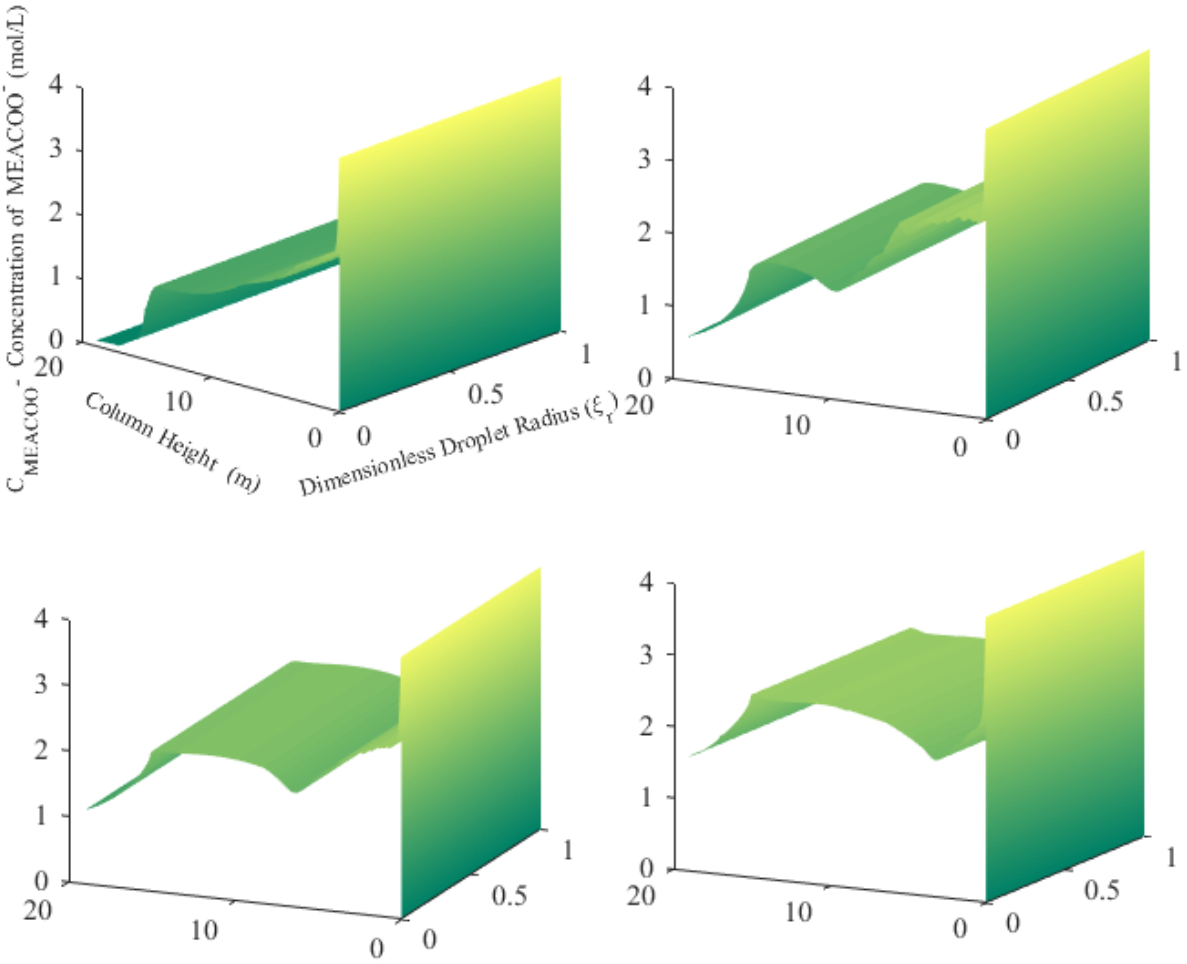

Figure 10: Case 1: Carbamate concentration profiles as a function of position for $c_N = 10^7$ droplets/cm^3 , Top row: (a) Flue gas 2, (b) Flue gas 2, Bottom row: (c) Flue gas 3 (d) Flue gas 4.

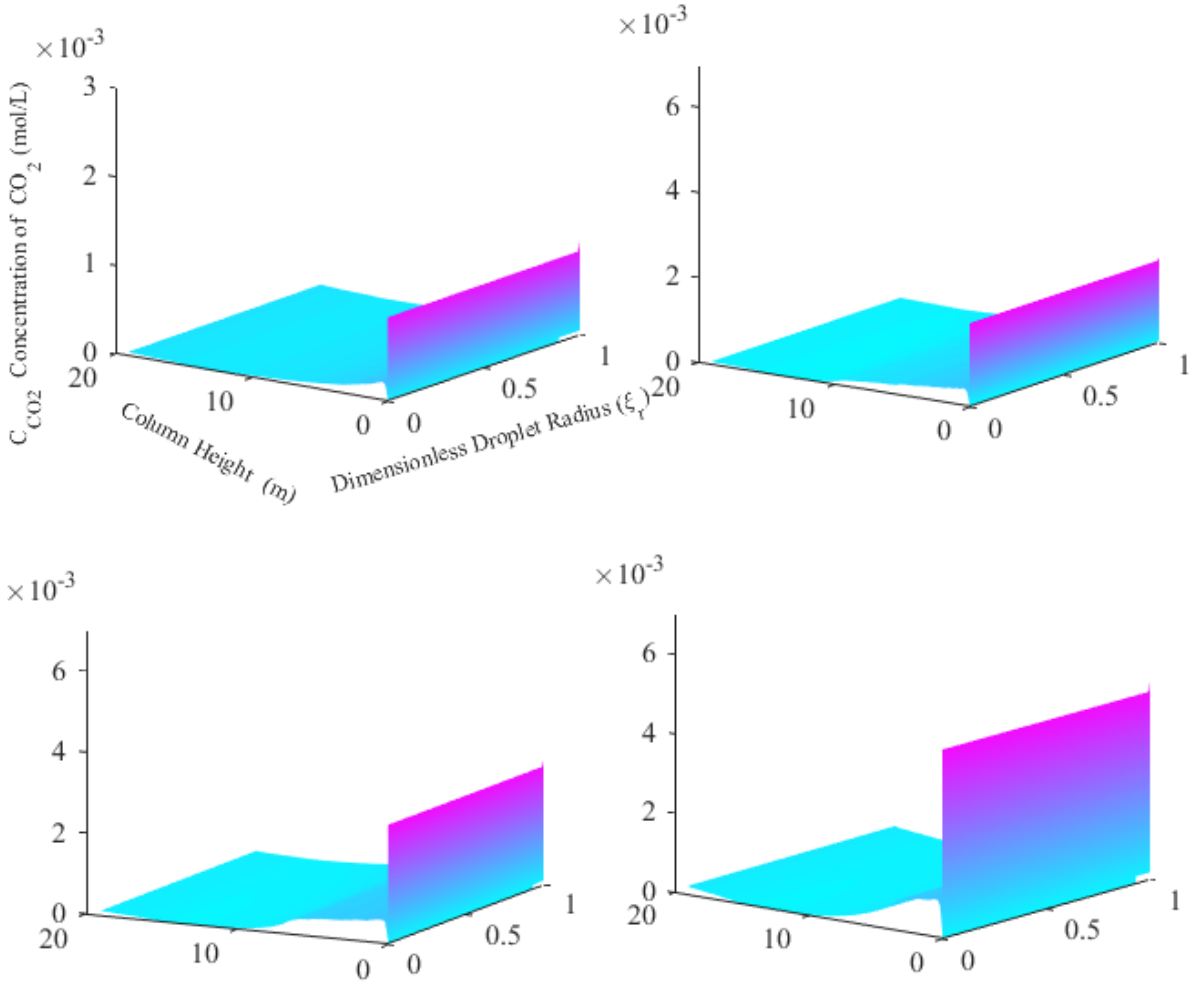

Figure 11: Case 1: CO_2 concentration profiles as a function of position for $c_N = 10^7$ droplets/cm^3 , Top row: (a) Flue gas 1, (b) Flue gas 2, Bottom row: (c) Flue gas 3 (d) Flue gas 4

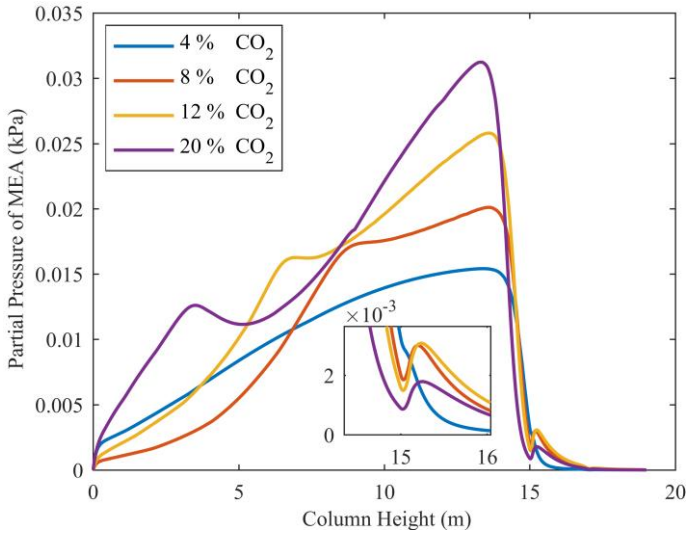

Figure 12: Case 1: Gas phase MEA partial pressure profiles for $c_N = 10^7$ droplets/cm^3

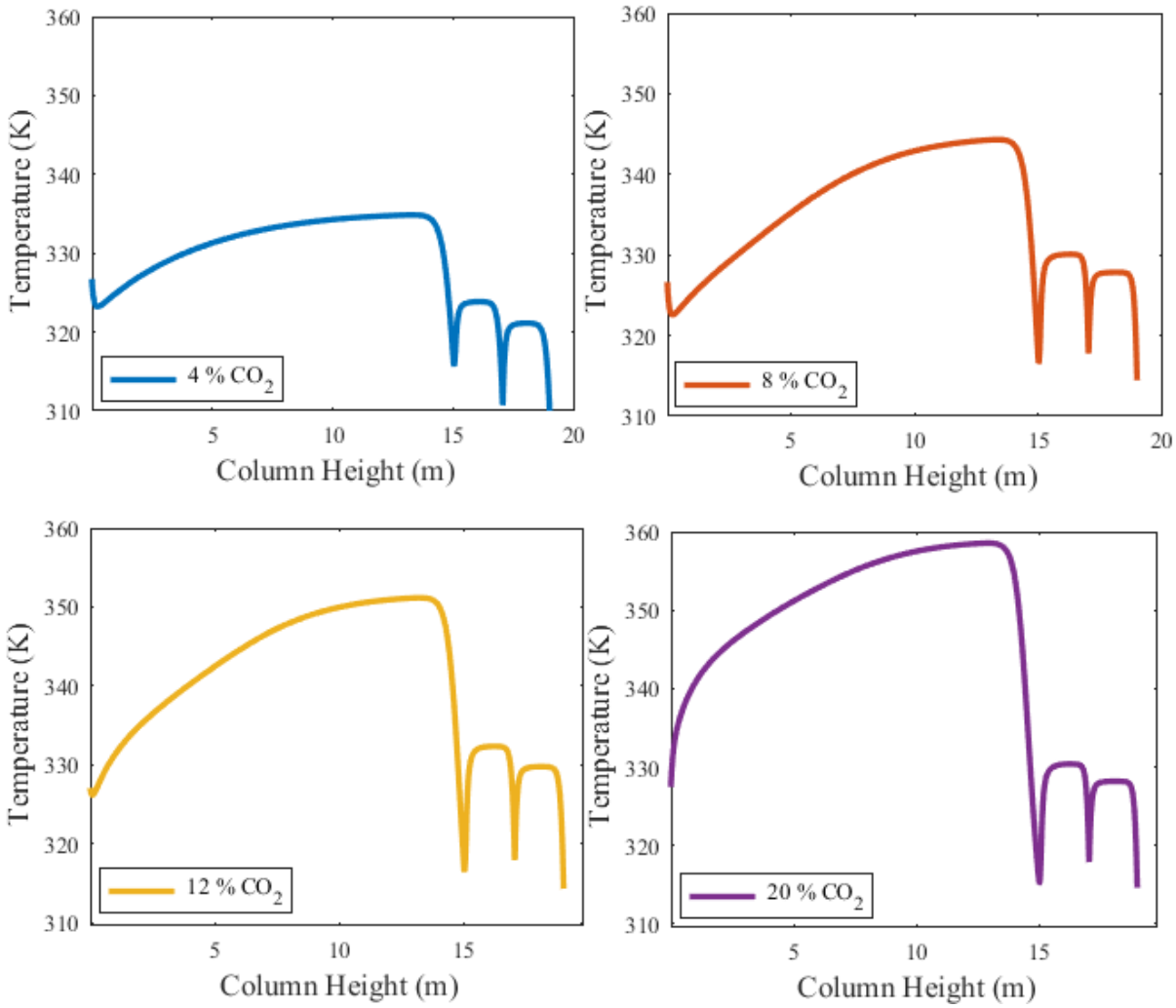

Figure 13: Case 1: Droplet temperature profiles as a function of position for $c_N=10^7$ droplets/cm^3

As is seen by comparing Figures 7 and 13, increasing droplet number concentration does not affect the temperature profiles significantly. These are governed by the bulk absorption of CO_2 which is much larger than the absorption into the droplet phase. As expected there is a strong influence of CO_2 concentration on the temperature profiles.

Case 2:

Case 2 is modelled to see the effect of initial composition of the aerosol droplets. For this case, with droplets initially containing 5M, the predicted profiles for 10^3-10^5-10^7 droplets/cm^3 are included as supplementary information.

With 10^3 droplets/cm^3, the free MEA, CO_2 and carbamate profiles are shown in Figures S4, S5 and S6 and the gas phase MEA profile in Figure S7. 1 and 1000 droplets/cm^3 behave the same so only one is shown. From Figure S4, it is seen that liquid phase free MEA starts decreasing instantly from the droplet as it enters the absorber. Simultaneously carbamate builds up. What happens is that CO_2 diffuses rapidly into the droplets and reacts. Strong radial CO_2 gradients are seen in this case for all flue gas types, but particularly for flue gas 4.

Further up in the column the free MEA and carbamate levels become more and more like the ones in Case 1, but more carbamate is formed in Case 2 toward the absorber top.

For droplet number concentrations 10^5 and 10^7 droplets/cm^3, the composition profiles are shown in Figures S8-S13. The gas phase MEA profiles for 10^7 droplets /cm^3 are presented in Figure S14. The initial increase in gas phase MEA pressure shown in the zoomed figure is because of desorption of MEA from the droplets when the volume of incoming droplets is large. As they enter the column, the liquid bulk is not able to absorb MEA fast enough. Temperature profiles are not included for Case 2 as the initial composition of the droplets does not affect the temperature profiles significantly for any number concentration.

Droplet growth for case 2 is shown in Figure S15. The profile characteristics are the same as seen in Figure 8. Preliminary reduction in size at the very bottom of the column is seen, because of MEA depletion at the bottom of the column as discussed earlier. For lower number concentrations the droplet growth in all flue gases is slightly higher than for Case 1, indicating a small effect of initial composition of the droplet on growth.

Effect of Intercooling:

Intercooling in CO_2 absorption systems is considered as a feasible method to improve solvent absorption capacity and effective mass transfer in CO_2 absorption processes. The effect of absorber intercooling on overall energy requirement will also depend on other factors such as lean amine loading and L/G ratio. We have seen that increased inlet gas CO_2 content leads to higher carry-over of amine into the water wash and it is also reported that varying the parameters of either the absorption column or water wash system may help to reduce the amine emissions (Majeed and Svendsen, 2017).

(Karimi et al., 2011) studied the effect of intercooling in an absorption system based on MEA. They proposed that the best location to insert intercooling is about a quarter of the absorber height from the bottom of the column.

With Type 4 flue gas, the temperature reaches above 80 ^{0}C at one point in the column. This leads to high MEA volatility and has a negative effect on aerosol carried emissions. New simulations in CO2SIM were performed to see the effect of intercooling on aerosol growth for this specific flue gas. The tower height is 15m and the intercooling, following the recommendation of (Karimi et al., 2011), was inserted 3.75m from the column. The lean solution entered at 40 ^{0}C as before, and the intercooling brought the liquid temperature back 40 ^{0}C. The bulk liquid phase profiles were extracted and used to model droplet growth. In this section, Flue gas 4 will be considered as base case to compare with the intercooling case.

In order to model this case in Matlab and to simplify, only one initial droplet composition was chosen i.e. pure water droplets with initial radius 0.15 μm. The results are presented for two different number concentrations: 10^3 and 10^7 droplets/cm^3. Free MEA, carbamate and CO_2 profiles for these number concentrations are shown in Figure 14. The temperature profiles are presented in Figure 16.

The build-up of MEA and carbamate inside the droplets is qualitatively very similar to what was seen previously for flue gas 4. However, for 10^3 droplets/cm^3 it is seen that the build-up of carbamate and MEA inside the droplet at the exit of the absorber is higher than for the base case. As the droplets leave the absorber they contain around 2 mol/L and 1.1 mol/L of free MEA and carbamate respectively. This indicates higher transfer of MEA from the gas phase to the droplets and this is also reflected in the lower partial pressure of MEA in the gas phase as shown in Figure 15a. With a droplet number concentration of 10^7 droplets/cm^3, the MEA content inside the droplets is still higher than for the base case with flue gas 4 and reaches 1.15 mol/L while carbamate formation is slightly less than in the base case. This is reasonable with the lower partial pressure of MEA in the gas phase as shown in Figure 15b.

For the water wash inlet we see that in flue gas 4, base case, the droplets contain carbamate (1.65mol/L) and less free MEA (0.98mol/L). When the droplets leave the second water wash with the treated flue gas, there is still carbamate present inside the droplets (0.25mol/L). With intercooling, the droplets enter the water wash containing significant amounts of free MEA (2 mol/L) and less carbamate (1.1mol/L). In this case the water wash is able to remove extensively both the free MEA and the carbamate present inside the droplets. With 10^3 droplets/cm^3 the treated flue gas droplets at the exit of the second wash contain only 0.05mol/L of free MEA and 0.08 mol/L of carbamate.

This indicates a significant reduction in both free MEA and carbamate caused by the lower water wash inlet temperature than in the base case. This holds true for 10^7 droplets/cm^3 as well.

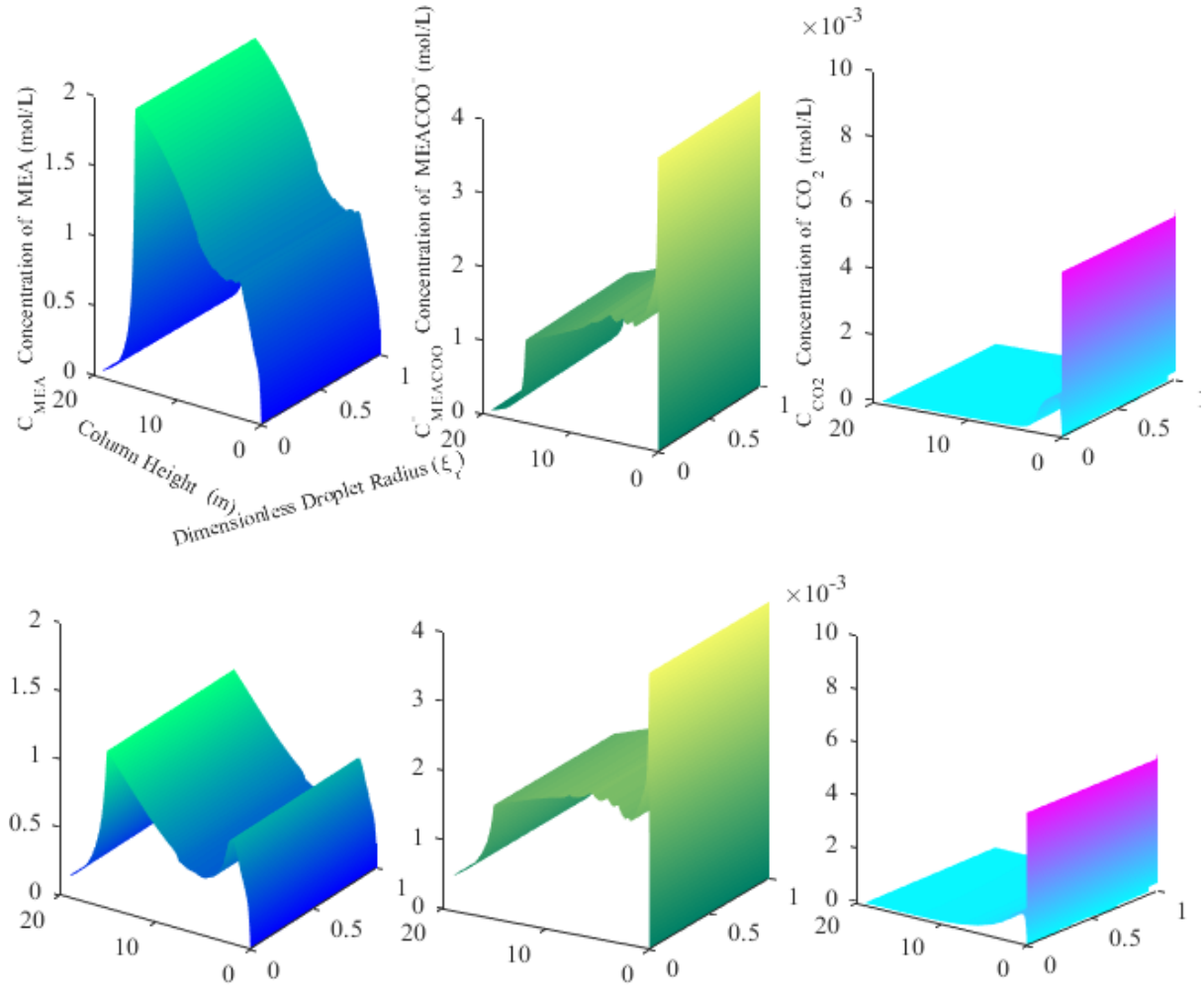

Figure 14: Top row: (a) Free MEA concentration profiles, c_N= 10^3droplets/cm^3, (b) Carbamate concentration profiles, c_N= 10^3droplets/cm^3 (c) CO_2 concentration profiles, c_N= 10^3droplets/cm^3 , Bottom row: (d) Free MEA concentration profiles, c_N= 10^7droplets/cm^3, (e) Carbamate concentration profiles, c_N= 10^7droplets/cm^{3,} (f) CO_2 concentration profiles, c_N= 10^7droplets/cm^3.

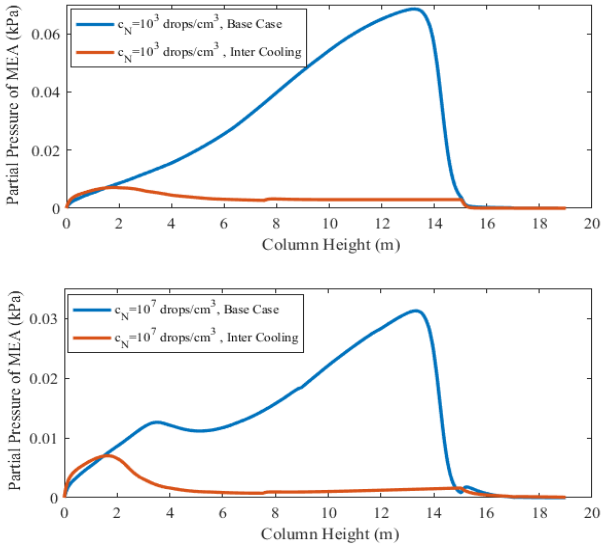

Figure 15: Gas phase MEA partial pressure profile (a) c_N= 10^3droplets/cm^3, (b) c_N= 10^7droplets/cm^3

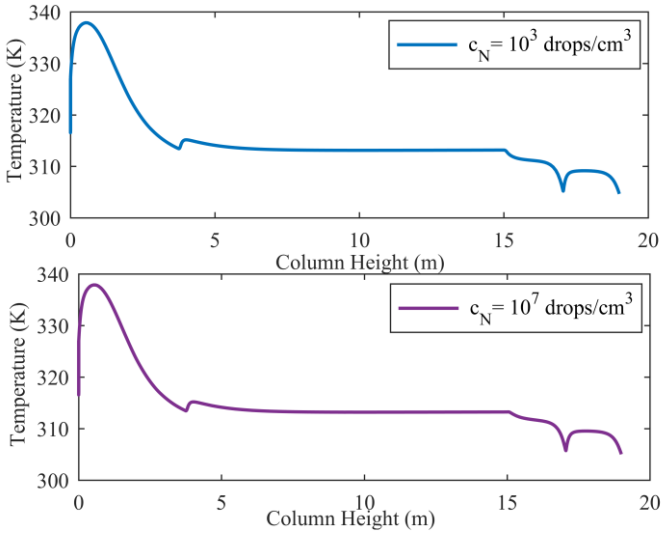

Figure 16: Droplet temperature profiles as a function of position

Droplet growth is significantly reduced when intercooling is used as seen in Figure 17 for both number concentrations. The droplets grow in the water wash section because of water condensation. When comparing both droplet number concentrations in the intercooling case, the growth is seen to be only slightly affected by the droplet number concentration.

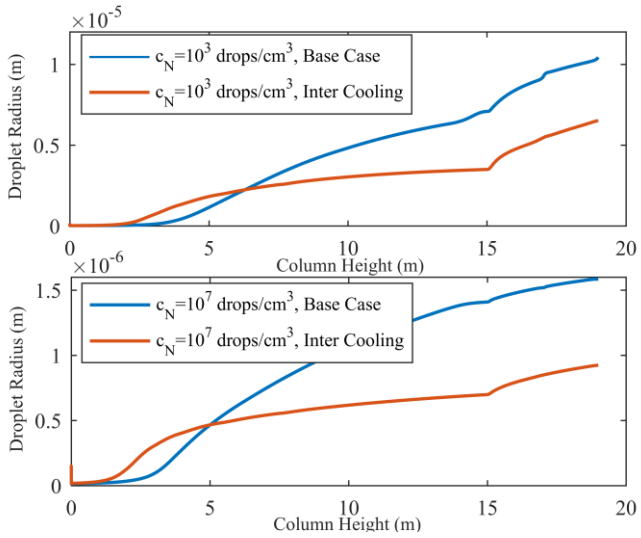

Figure 17: Growth of aerosol droplet

Results assessment and validation:

A few experimental investigations and pilot campaign results exist that show particle number concentration and estimation of amine emissions based on aerosols. These studies only go up to maximum 12% of CO_2 in the flue gas. Unfortunately, parameters like initial droplet size and inlet droplet composition are not given in these campaigns. Most of the campaigns deal with external fed nuclei.

To perform a direct result assessment based on these experimental investigations is not possible, but still they can be used for an overall evaluation of the present model.

The modelling results in this work are based on droplets having an initial size of 0.15µ with different particle number concentrations and different initial composition. We chose this size and number concentrations of 10^3-10^7 droplet/cm^3, as this is the number range and size of aerosols droplets reported in literature. Four different flue gas sources were compared in this work and estimated amine emissions right after the absorber and after the second water wash are presented in Table 2 and Table 3. For a detail analysis of case 1, emissions throughout the column and water washes are plotted in Figure 18.

Table 2: Amine emission from all flue gas sources in mg/Nm^3 (Case 1)

	c_N= droplets/cm^3	Flue Gas 1	Flue Gas 2	Flue Gas 3	Flue Gas 4
Absorber Top	10^3-10^7	0.15 - 266	11 - 7700	84 - 22000	388-53000
Water Wash 2 Top	10^3-10^7	0.1-93	4 - 5300	31 -18000	200-45000

Table 3: Amine emission from all flue gas sources in mg/Nm^3 (Case 2)

	c_N= droplets/cm^3	Flue Gas 1	Flue Gas 2	Flue Gas 3	Flue Gas 4
Absorber Top	10^3-10^7	5 - 5000	50 - 15000	160 - 31000	520 - 59000
Water Wash 2 Top	10^3-10^7	0.9 - 3400	18 - 11000	65 - 24000	300 - 50000

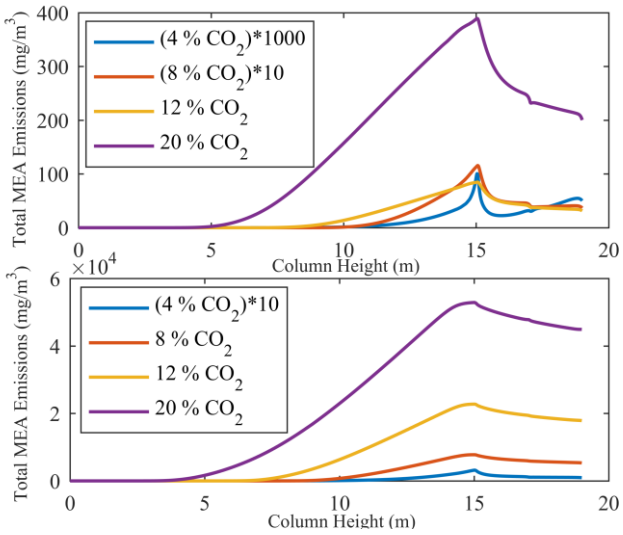

Figure 18: Case 1: Estimated amine emissions from modelled absorber and water wash column (a) c_N=10^3 droplets/cm^3 , (b) c_N=10^7 droplets/cm^3

It is evident from these results that as the CO_2 content in the flue gas increases, the aerosol based amine emissions increase. The results also show the effectiveness of the water wash section in reducing the total amine emissions from typical PCCC plants and results are in agreement with (Majeed and Svendsen, 2017). These emissions can further be reduced by altering the operating parameters of either the absorption section or the water wash as discussed earlier in the intercooling section.

Varying the initial composition of the inlet droplets has a strong impact on the total amine emissions, see Table 3.

The results presented here are in line with the findings of modelling work presented in (Khakharia et al., 2014b), where increasing CO_2 content in the flue gas was found to increase amine emission. However, the estimated emissions in (Khakharia et al., 2014b) were generally lower than in the current model. This may be because the model presented in that work is simplified and because the total height of their column was only 2m, giving less time for droplet growth.

Case 1 and flue gas 4 in which the content of CO_2 is 20% was chosen to implement intercooling. To sum up the results for the base case and intercooling case the predicted results are shown in Figure 19 indicating the effectiveness off intercooling in reducing amine emissions from absorption columns. It is seen that the effect is really significant such that intercooling does not only have an effect on energy use, but also a positive effect on aerosol emissions.

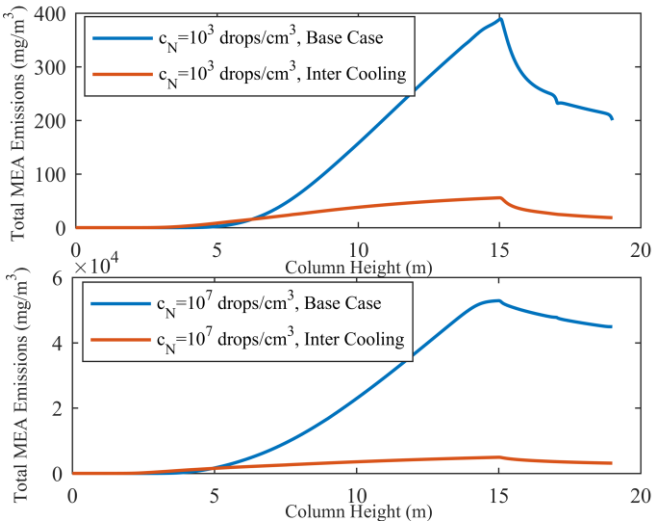

Figure 19: Estimated amine emissions from modelled absorber and water wash column

Conclusions:

A detailed characterization of aerosol growth in absorption processes is needed to avoid prohibitive amine emissions from PCCC plants. The present work provides an overview of amine emissions from large CO_2 emitting sources as well as a model for characterization of aerosol droplet in terms of composition and temperature. This work is aimed at understanding aerosol based emissions for different sources and what countermeasures can be taken for the individual flue gas type to reduce emissions.

Four different atmospheric flue gases were modelled in this work, ranging from 4-20% in CO_2 content. Inlet droplets of size 0.15µ with initial concentration 0 and 5M MEA were tested in number concentrations from $1 – 10^7$ droplets/cm^3. For 20% CO_2, the effect of intercooling was studied.

The aerosol droplets grow from their initial size regardless of their initial composition and type of flue gas processed. The initial composition of the droplet has a significant effect on emissions as seen in case 2.

With increasing CO2 concentration, more carbamate is formed relative to free MEA. This leads to less effective water wash and significantly higher final emissions, from 0.15 to 200 mg/Nm^3 for 1000 droplets/cm^3 and from 200 to 45000 mg/Nm^3 with 10^7 droplets/cm^3.

With 1000 droplets/cm^3, no visible depletion of MEA in the absorber and water wash sections was found for any of the CO_2 concentrations. However, at 20% CO_2, the droplet growth was reduced compared to a single droplet, indication that some gas phase MEA depletion had occurred.

At 10^7 droplets/cm^3, gas phase MEA partial pressure changes are clearly seen. With 4% CO_2 this only happens in the water wash, whereas for the higher contents the effect starts lower and lower down in the absorber.

The carry-over of amine into the water wash increases with increasing gas phase CO_2 content. However, the effect on the gas phase MEA content in the water wash goes through a maximum caused by strong carbamate formation with 20% CO_2 in the inlet flue gas, giving low free MEA and less rapid release into the water wash gas phase.

The droplet temperature profiles are unaffected by number concentration and initial composition of aerosol droplets.

It is found that the water wash section reduces significantly the aerosol based, and thereby the total amine emissions. The effect of the water wash is reduced when the flue gas CO_2 content increases.

Intercooling lowers the partial pressure of MEA in both absorber and water wash significantly. This reduces the droplet growth, but not as much as would intuitively be expected from the reduction in MEA partial pressure. Intercooling reduces MEA emissions drastically and, in the case of 20% CO_2 in the flue gas, by a factor of 5-10.

Acknowledgement

Financial support from the Faculty of Natural Sciences at the Norwegian University of Science and Technology, Trondheim is greatly appreciated.

Notations

P	Partial pressure (kPa)	**Greek letters**	
t	Time (sec)		
T	Temperature (K)	μ	μm
Indices		**Figure captions**	
MEA	Monoethanol amine	ABS	Absorber
$MEACOO^-$	Carbamate	WW1 (1,2,3,4)	Water circulation in water wash 1
CO_2	Carbon dioxide	WW2 (1,2,3,4)	Water circulation in water wash 2
d	Droplet/Aerosol	Gas (1,2,3,4,5)	Flue gas entering and leaving absorber and water washes
g	Gas	Solvent (1,2)	Solvent entering and leaving absorber
l	Liquid	WW_bleed	Bleed stream from water wash
		Div (01, 01)	Stream dividers
		Flash (01,02)	Flash tanks
		Mix (01,02)	Mixers

References:

Abu-Zahra, 2009. Carbon dioxide capture from flue gas: development and evaluation of existing and novel process concepts (PhD Thesis). Technical University of Delft, The Netherlands.

Einbu, A., 2016. CO2SIM (Flowsheet Simulator for CO2 Absorption Processes) [WWW Document]. SINTEF. URL https://www.sintef.no/en/software/co2sim-flowsheet-simulator-for-co2-absorption-proc/ (accessed 4.11.17).

Fulk, S.M., 2016. Measuring and modeling aerosols in carbon dioxide capture by aqueous amines (Thesis).

Global CCS Institute, 2013. Capturing CO2 from gas or coal power generation- what's the difference? | Global Carbon Capture and Storage Institute [WWW Document]. URL https://www.globalccsinstitute.com/insights/authors/dennisvanpuyvelde/2013/11/06/capturing-co2-gas-or-coal-power-generation-what%E2%80%99s (accessed 4.5.17).

IEA, 2016. Key world energy statistics (KWES). International Energy Agency.

IEAGHG, 2010. Environmental Impacts of Amine Emissions During Post Combustion Capture Workshop.

IEAGHG, 2008. CO2 capture in cement industry (A technical study) (No. 2008/3).

IPCC, 2005. IPCC Special report on Carbon Dioxide Captuer and Storage (SRCCS).

Kang, J.-L., Zhang, Y., Fulk, S., Rochelle, G.T., 2017. Modeling Amine Aerosol Growth in the Absorber and Water Wash. Energy Procedia, 13th International Conference on Greenhouse Gas Control Technologies, GHGT-13, 14-18 November 2016, Lausanne, Switzerland 114, 959–976. doi:10.1016/j.egypro.2017.03.1241

Karimi, M., Hillestad, M., Svendsen, H.F., 2011. Investigation of intercooling effect in CO2 capture energy consumption. Energy Procedia, 10th International Conference on Greenhouse Gas Control Technologies 4, 1601–1607. doi:10.1016/j.egypro.2011.02.030

Khakharia, P., Brachert, L., Mertens, J., Anderlohr, C., Huizinga, A., Fernandez, E.S., Schallert, B., Schaber, K., Vlugt, T.J.H., Goetheer, E., 2015. Understanding aerosol based emissions in a Post Combustion CO2 Capture process: Parameter testing and mechanisms. Int. J. Greenh. Gas Control 34, 63–74. doi:10.1016/j.ijggc.2015.01.001

Khakharia, P., Kvamsdal, H.M., da Silva, E.F., Vlugt, T.J.H., Goetheer, E., 2014a. Field study of a Brownian Demister Unit to reduce aerosol based emission from a Post Combustion CO2 Capture plant. Int. J. Greenh. Gas Control 28, 57–64. doi:10.1016/j.ijggc.2014.06.022

Khakharia, P., Mertens, J., Vlugt, T.J.H., Goetheer, E., 2014b. Predicting Aerosol Based Emissions in a Post Combustion CO2 Capture Process Using an Aspen Plus Model. Energy Procedia 63, 911–925. doi:10.1016/j.egypro.2014.11.101

Knudsen, J.N., Bade, O.M., Askestad, I., Gorset, O., Mejdell, T., 2014. Pilot Plant Demonstration of CO2 Capture from Cement Plant with Advanced Amine Technology. Energy Procedia, 12th International Conference on Greenhouse Gas Control Technologies, GHGT-12 63, 6464–6475. doi:10.1016/j.egypro.2014.11.682

Knudsen, S., Randall, S., 2009. Amine Emissions to Air During Carbon Capture. Phase 1: CO2 and Amines Screening Study for Effects to the Environment. NILU Report. www.CO2.nilu.no.

Luo, X., Knudsen, J.N., de Montigny, D., Sanpasertparnich, T., Idem, R., Gelowitz, D., Notz, R., Hoch, S., Hasse, H., Lemaire, E., Alix, P., Tobiesen, F.A., Juliussen, O., Köpcke, M., Svendsen, H.F., 2009. Comparison and validation of simulation codes against sixteen sets of data from four different pilot plants. Energy Procedia, Greenhouse Gas Control Technologies 9 1, 1249–1256. doi:10.1016/j.egypro.2009.01.164

MacDowell, N., Florin, N., Buchard, A., Hallett, J., Galindo, A., Jackson, G., Adjiman, C.S., Williams, C.K., Shah, N., Fennell, P., 2010. An overview of CO2 capture technologies. Energy Environ. Sci. 3, 1645. doi:10.1039/c004106h

Majeed, H., Knuutila, H., Hillestad, M., Svendsen, H.F., 2017a. Gas phase amine depletion created by aerosol formation and growth. Int. J. Greenh. Gas Control 64, 212–222. doi:10.1016/j.ijggc.2017.07.001

Majeed, H., Knuutila, H.K., Hillestad, M., Svendsen, H.F., 2017b. Characterization and modelling of aerosol droplet in absorption columns. Int. J. Greenh. Gas Control 58, 114–126. doi:10.1016/j.ijggc.2017.01.006

Majeed, H., Svendsen, H.F., 2017. Effect of Water Wash on Mist and Aerosol Formation in Absorption Column. Chem. Eng. J. doi:10.1016/j.cej.2017.09.124

Mertens, J., Knudsen, J., Thielens, M.-L., Andersen, J., 2012. On-line monitoring and controlling emissions in amine post combustion carbon capture: A field test. Int. J. Greenh. Gas Control 6, 2–11. doi:10.1016/j.ijggc.2011.11.015

Moser, P., Schmidt, S., Stahl, K., Vorberg, G., Lozano, G.A., Stoffregen, T., Rösler, F., 2014. Demonstrating Emission Reduction – Results from the Post-combustion Capture Pilot Plant at Niederaussem. Energy Procedia, 12th International Conference on Greenhouse Gas Control Technologies, GHGT-12 63, 902–910. doi:10.1016/j.egypro.2014.11.100

Rochelle, G.T., 2009. Amine Scrubbing for CO2 Capture. Science 325, 1652–1654. doi:10.1126/science.1176731

Saha, C., Irvin, J.H., 2017. Real-time aerosol measurements in pilot scale coal fired post-combustion CO2 capture. J. Aerosol Sci. 104, 43–57. doi:10.1016/j.jaerosci.2016.11.005

Tobiesen, F.A., Hillestad, M., Kvamsdal, H., Chikukwa, A., 2012. A General Column Model in CO2SIM for Transient Modelling of CO2 Absorption Processes. Energy Procedia 23, 129–139. doi:10.1016/j.egypro.2012.06.071

Tobiesen, F.A., Svendsen, H.F., Juliussen, O., 2007. Experimental validation of a rigorous absorber model for CO2 postcombustion capture. AIChE J. 53, 846–865. doi:10.1002/aic.11133

Zhang, Y., Kang, J.-L., Fulk, S.M., Rochelle, G., 2017. Modeling Amine Aerosol Growth at Realistic Pilot Plant Conditions. Energy Procedia.

Supplementary Information

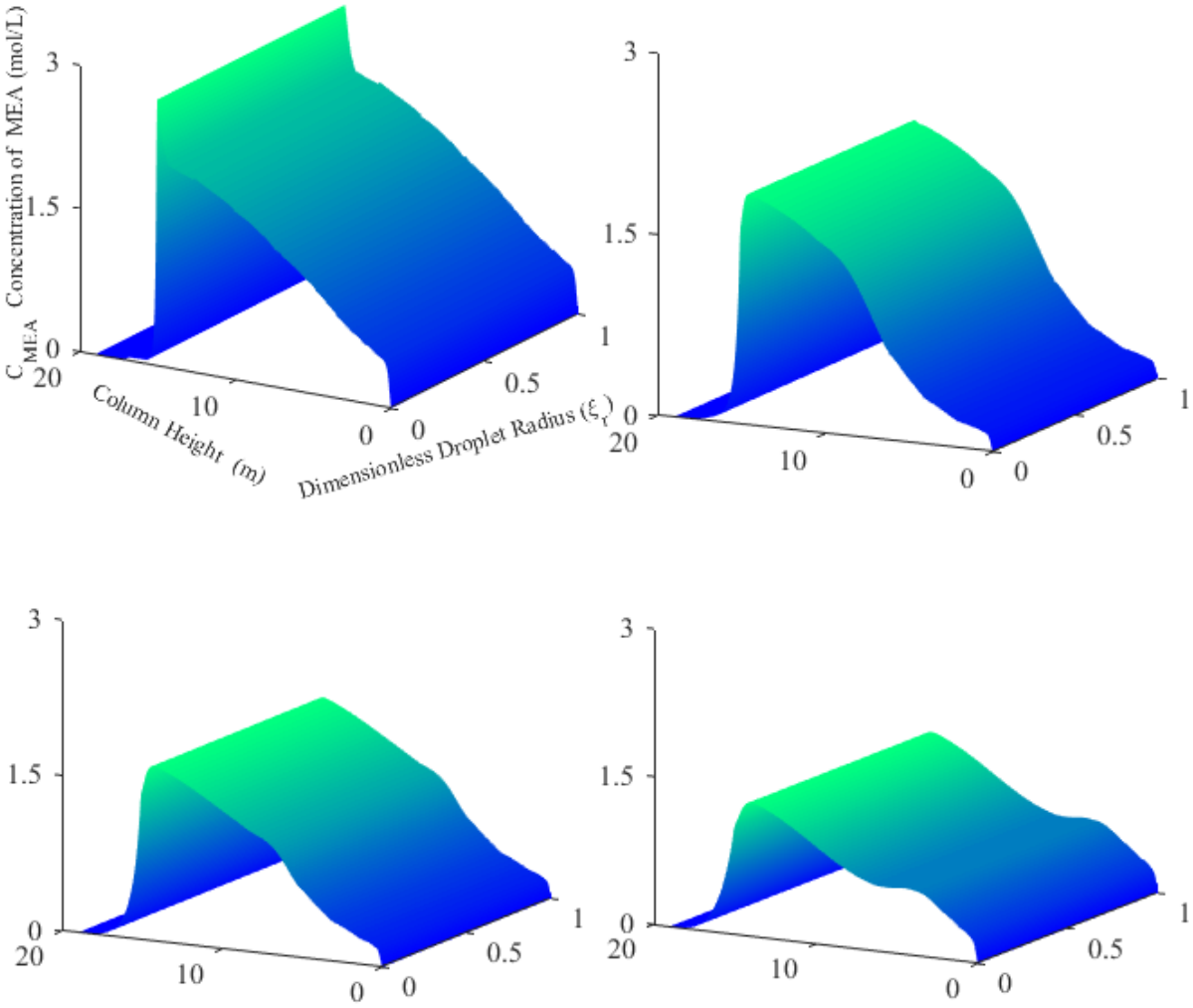

Figure S1: Case 1: Free MEA concentration profiles as function of position for $c_N = 10^5$ droplets/cm^3 (a) Flue gas 1, (b) Flue gas 2, (c) Flue gas 3 (d) Flue gas 4

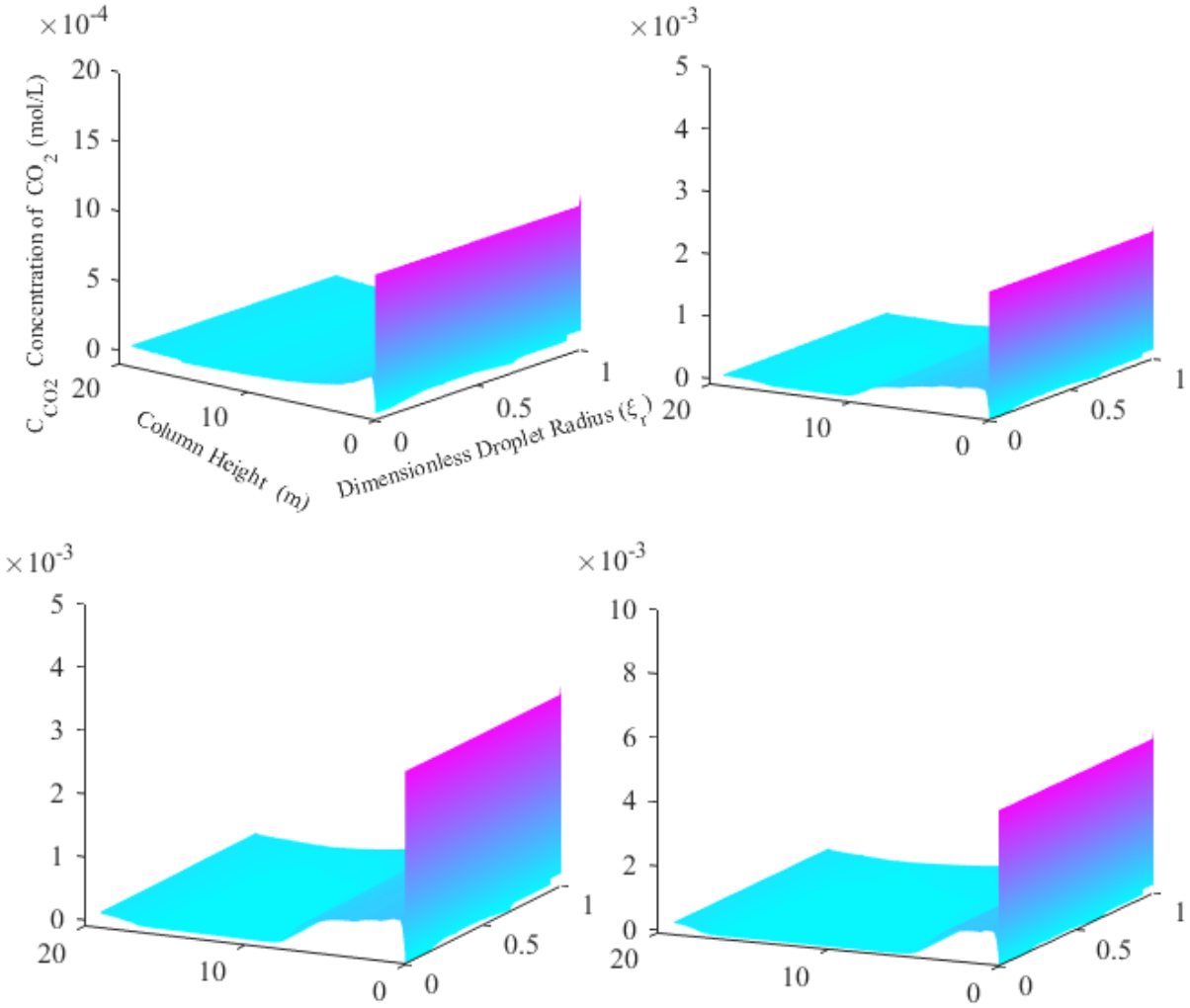

Figure S2: Case 1: CO_2 concentration profiles as function of position for $c_N = 10^5$ droplets/cm^3 (a) Flue gas 1, (b) Flue gas 2, (c) Flue gas 3 (d) Flue gas 4

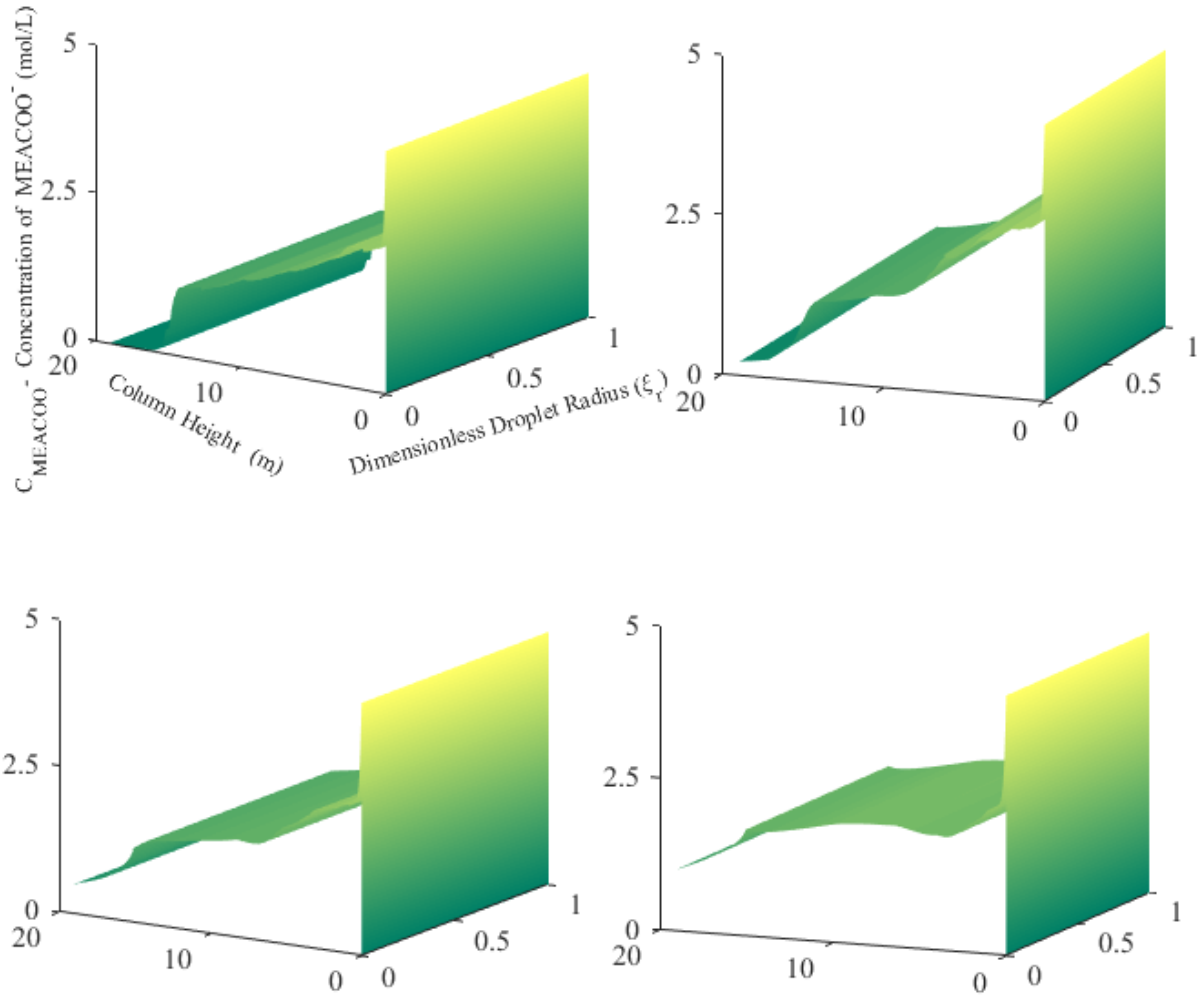

Figure S3: Case 1: Carbamate concentration profiles as function of position for c_N= 10^5 droplets/cm^3 (a) Flue gas 1, (b) Flue gas 2, (c) Flue gas 3 (d) Flue gas 4.

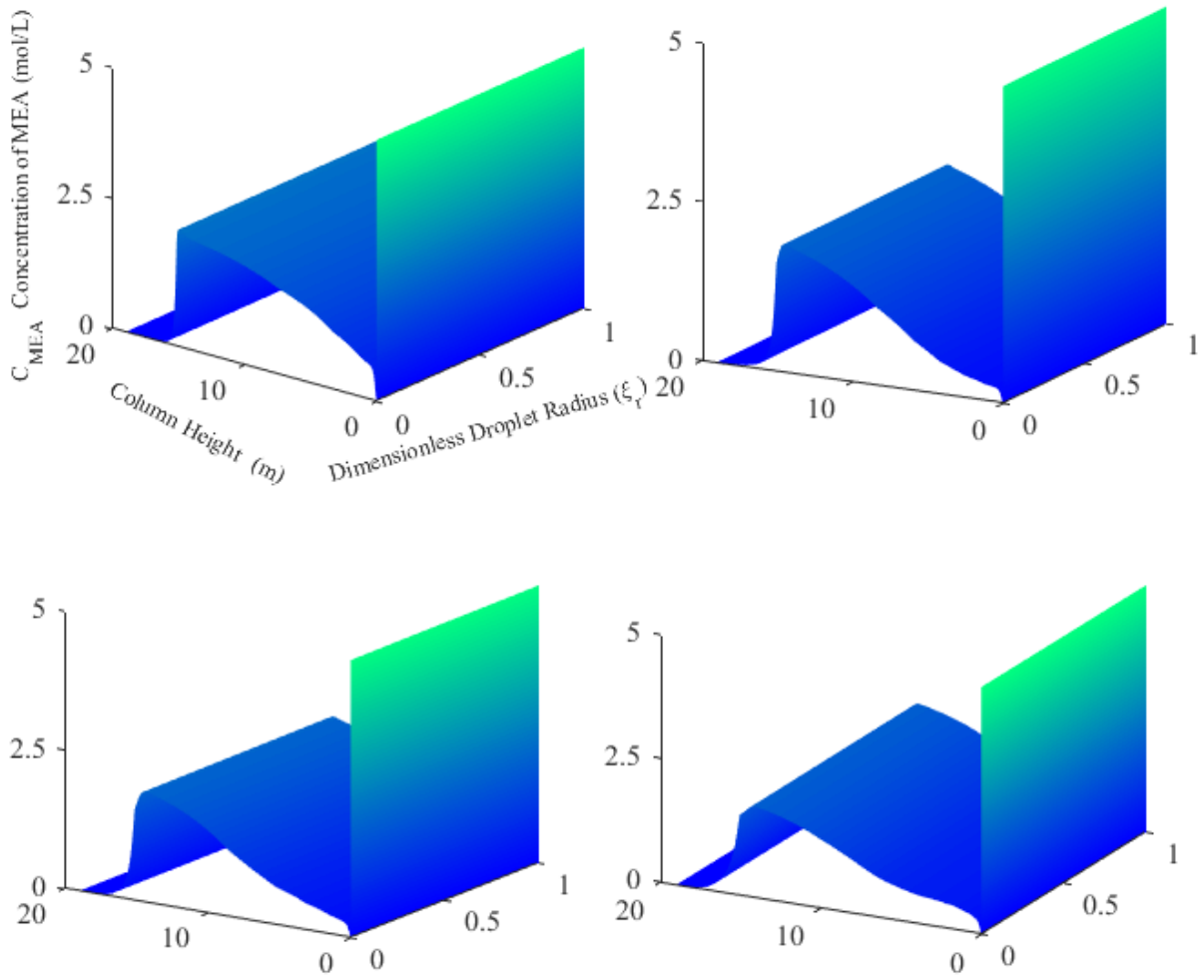

Figure S4: Case 2: Free MEA concentration profiles as function of position for $c_N = 10^3$ droplets/cm^3 (a) Flue gas 1, (b) Flue gas 2, (c) Flue gas 3 (d) Flue gas 4

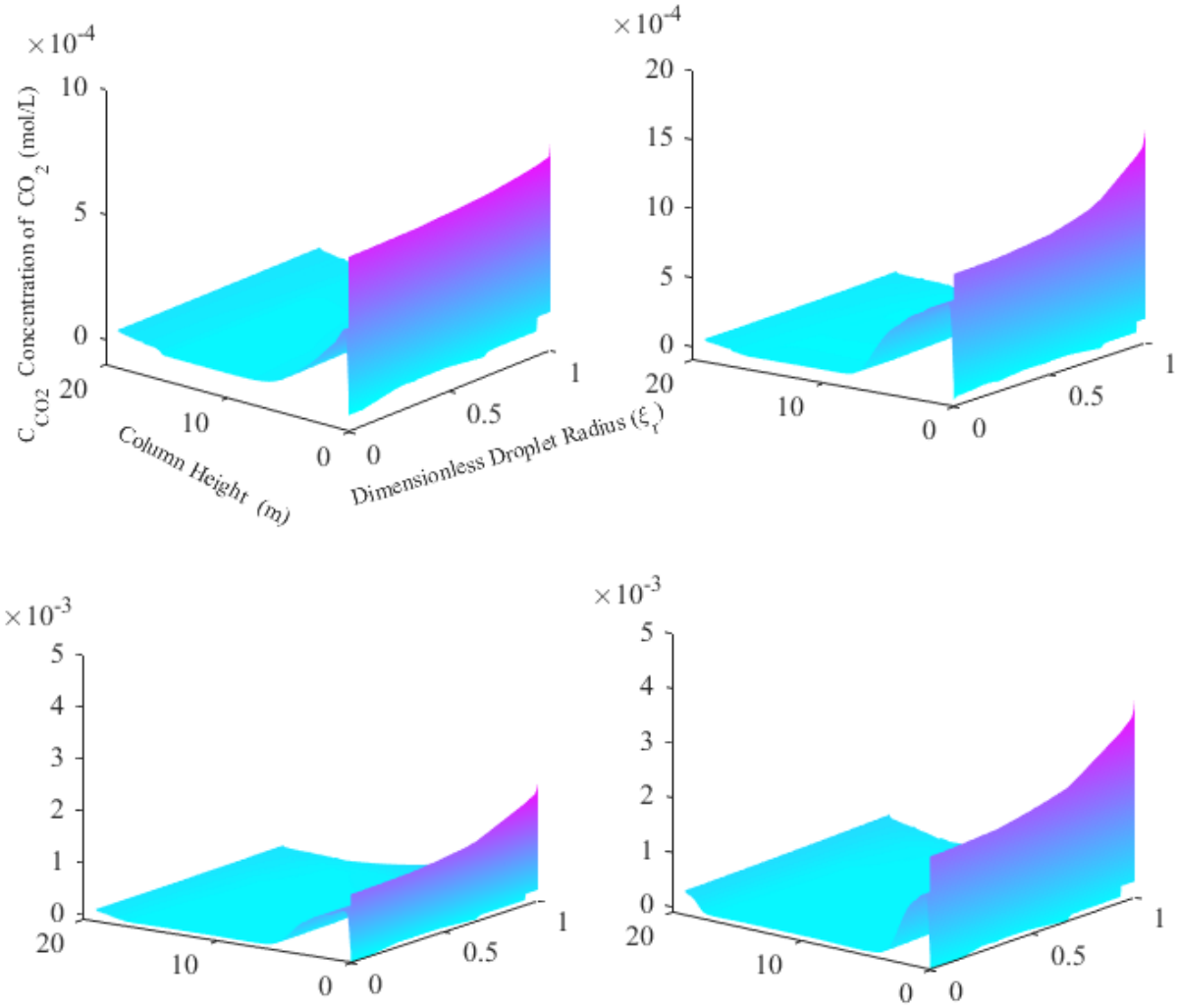

902

903 Figure S5: Case 2: CO_2 concentration profiles as function of position for $c_N = 10^3$
904 droplets/cm^3 (a) Flue gas 1, (b) Flue gas 2, (c) Flue gas 3 (d) Flue gas 4

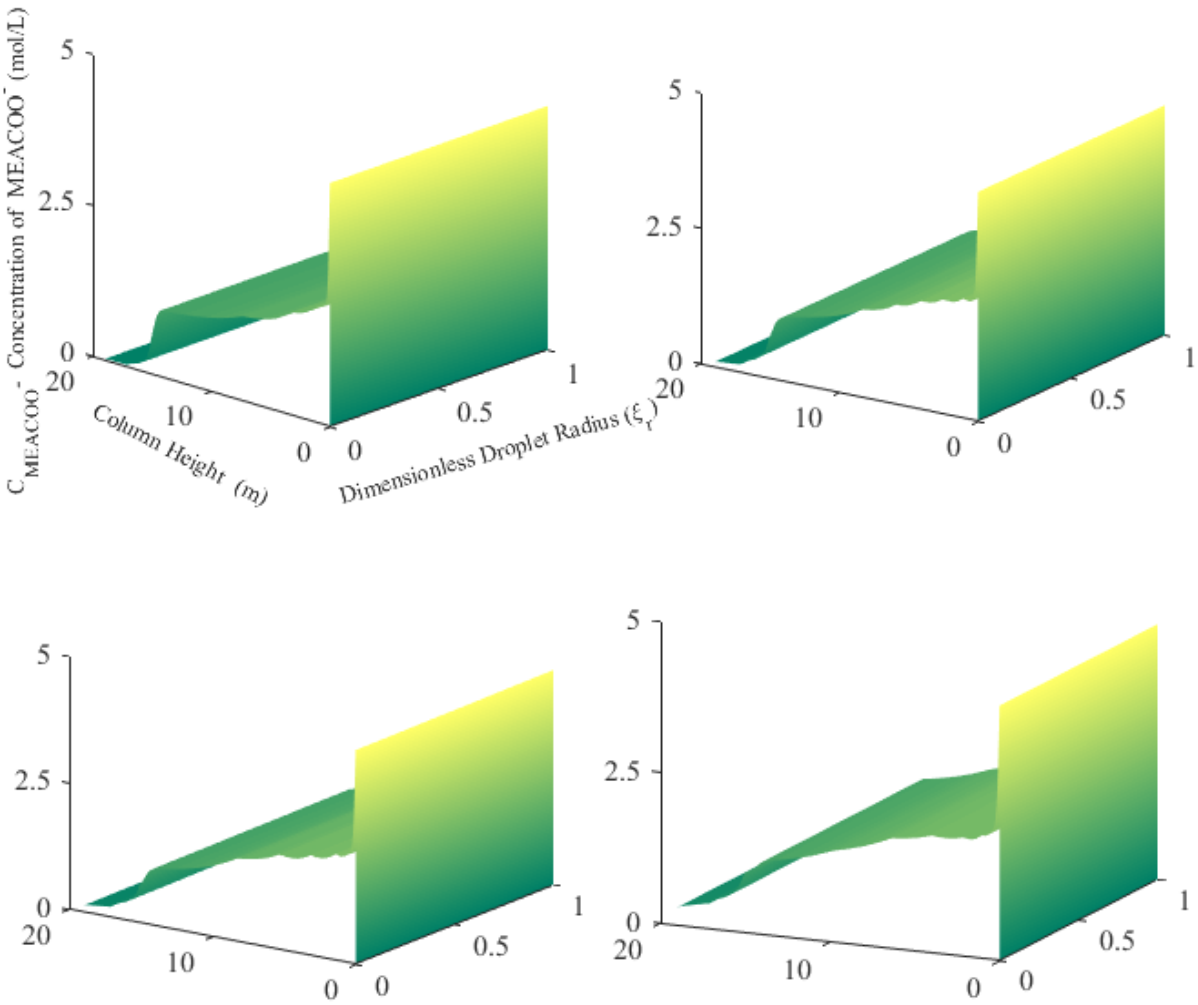

Figure S6: Case 2: Carbamate concentration profiles as function of position for $c_N = 10^3$ droplets/cm^3 (a) Flue gas 1, (b) Flue gas 2, (c) Flue gas 3 (d) Flue gas 4.

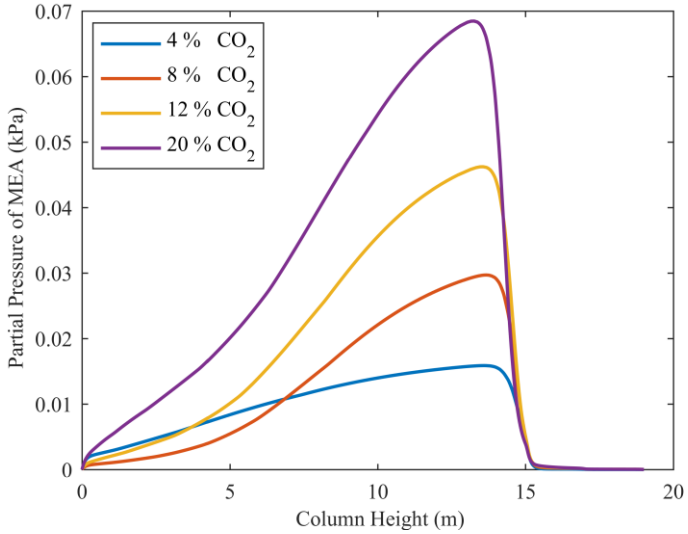

Figure S7: Case 2: Gas phase MEA partial pressure profiles for $c_N = 10^3$ droplets/cm^3

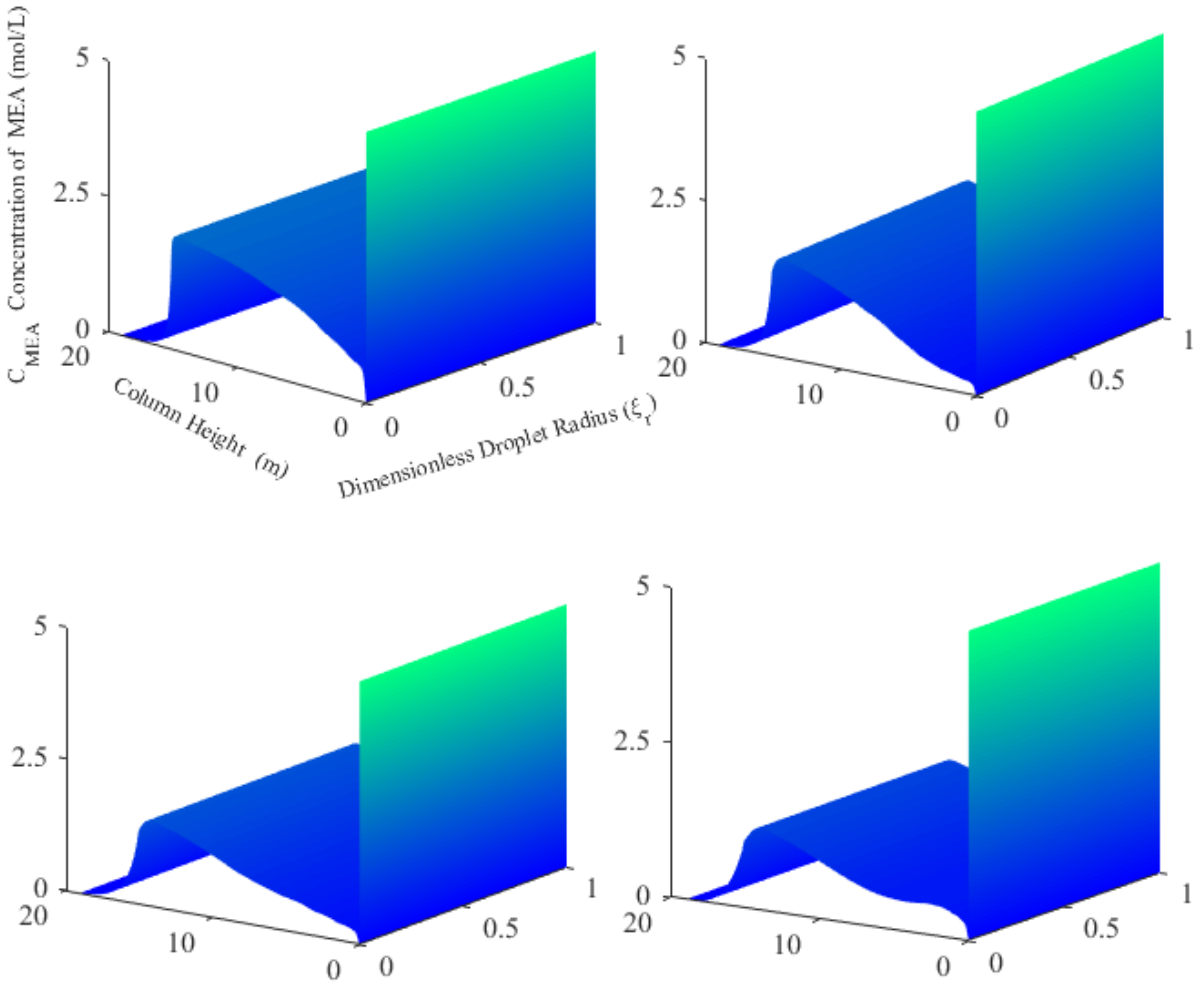

Figure S8: Case 2: Free MEA concentration profiles as function of position for $c_N = 10^5$ droplets/cm^3 (a) Flue gas 1, (b) Flue gas 2, (c) Flue gas 3 (d) Flue gas 4

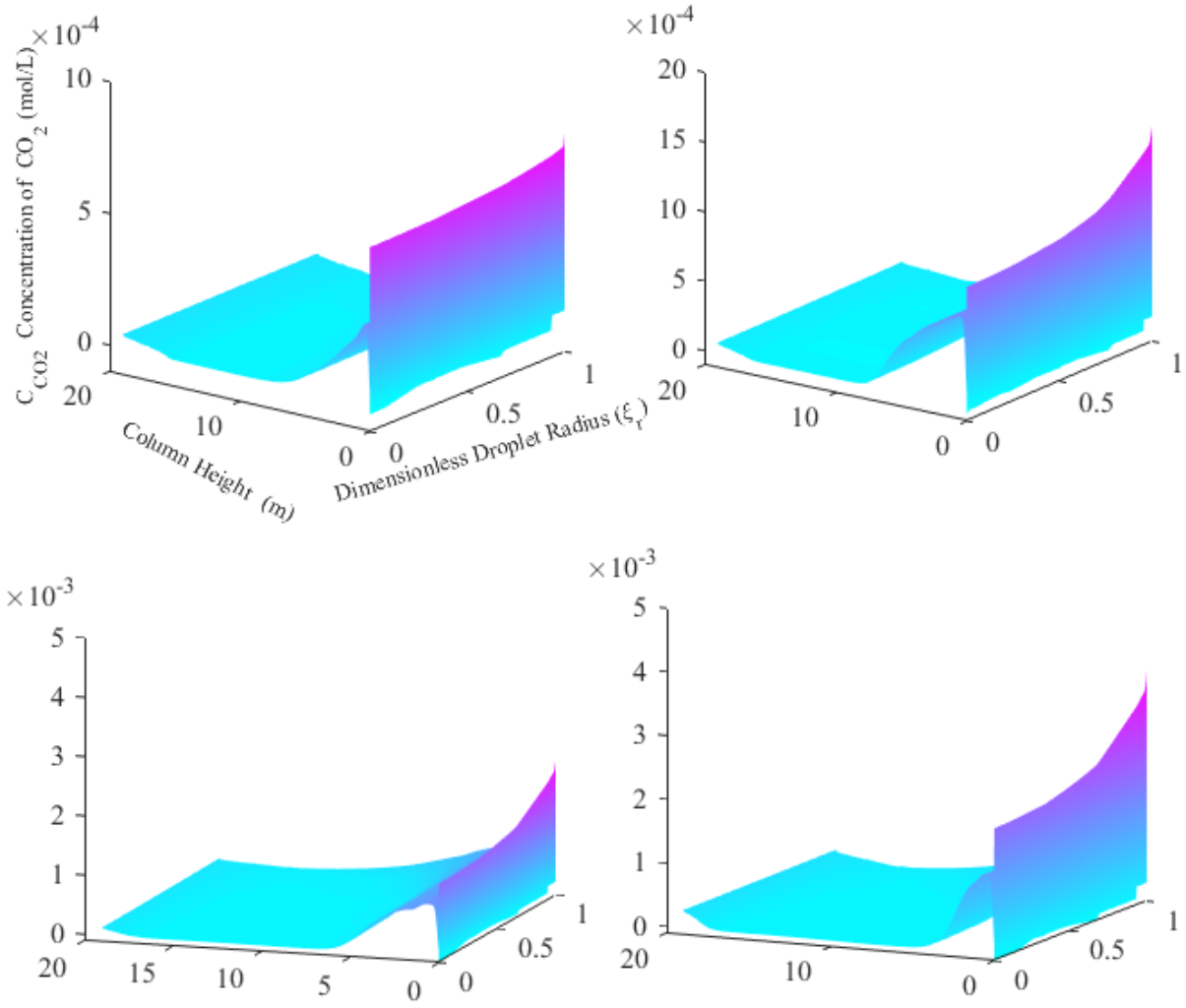

Figure S9: Case 2: CO_2 concentration profiles as function of position for $c_N = 10^5$ droplets/cm^3 (a) Flue gas 1, (b) Flue gas 2, (c) Flue gas 3 (d) Flue gas 4

928

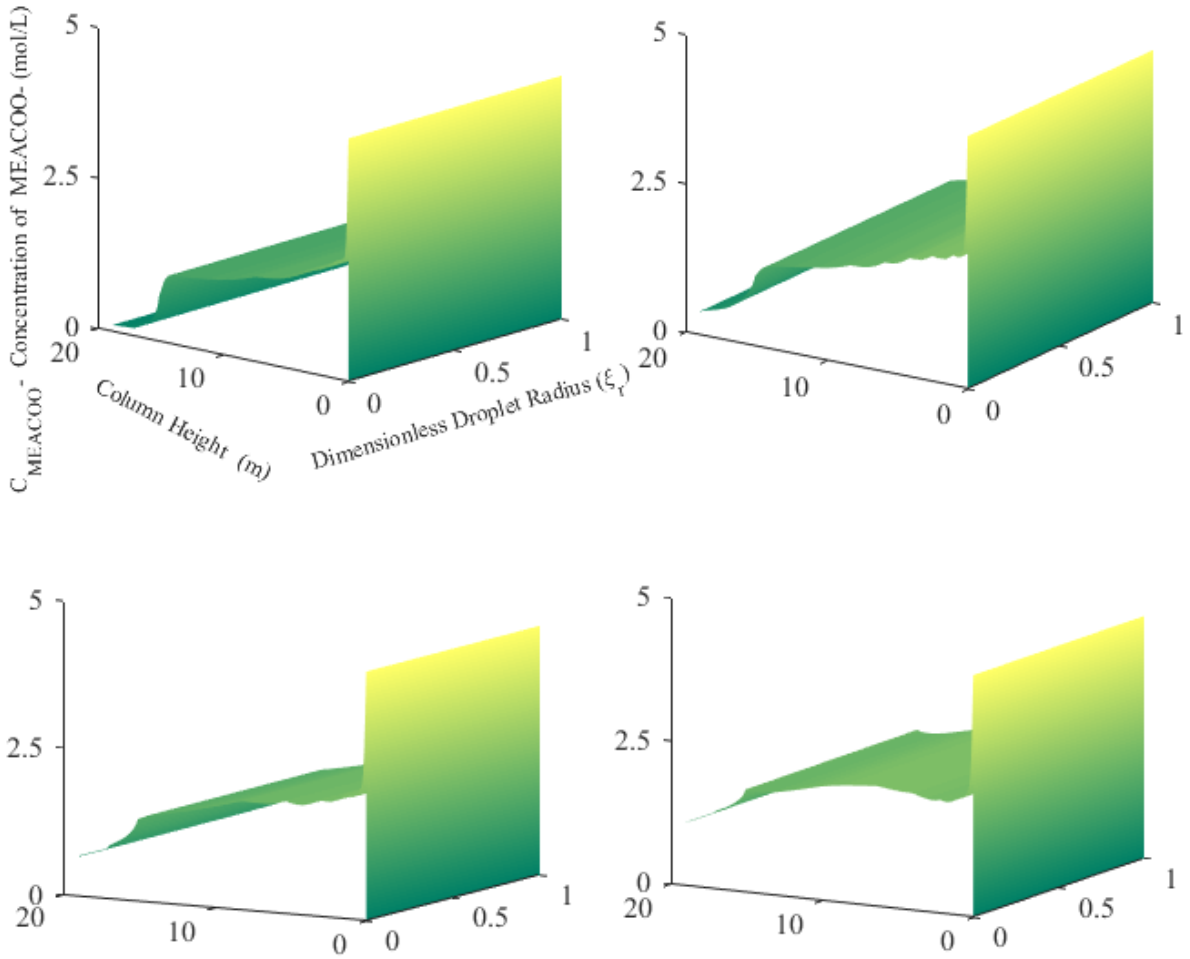

929

930

931 Figure S10: Case 2: Carbamate concentration profiles as function of position for $c_N = 10^5$
932 droplets/cm^3 (a) Flue gas 1, (b) Flue gas 2, (c) Flue gas 3 (d) Flue gas 4.

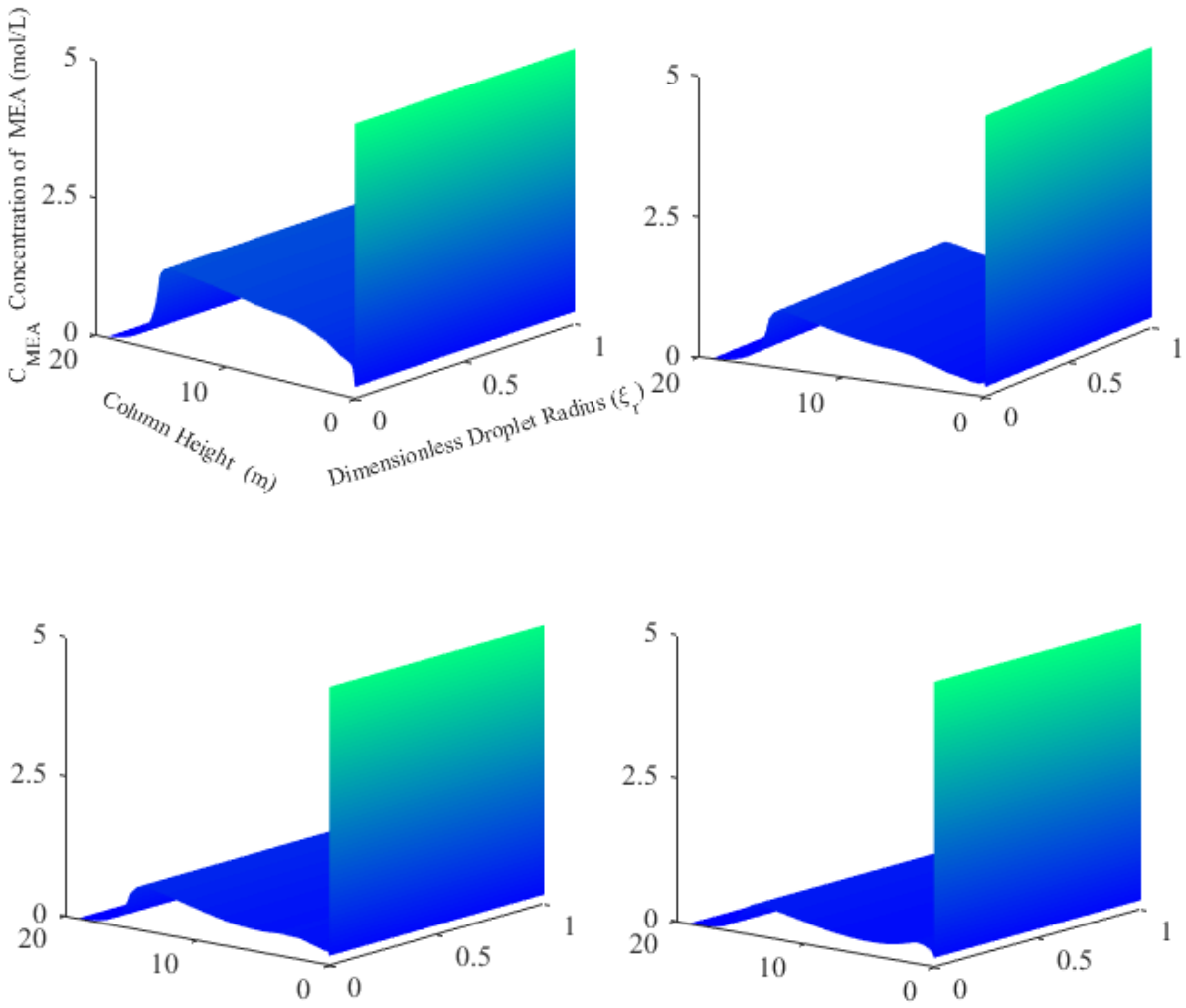

933

934

935 Figure S11: Case 2: Free MEA concentration profiles as function of position for $c_N = 10^7$
936 droplets/cm^3 (a) Flue gas 1, (b) Flue gas 2, (c) Flue gas 3 (d) Flue gas 4

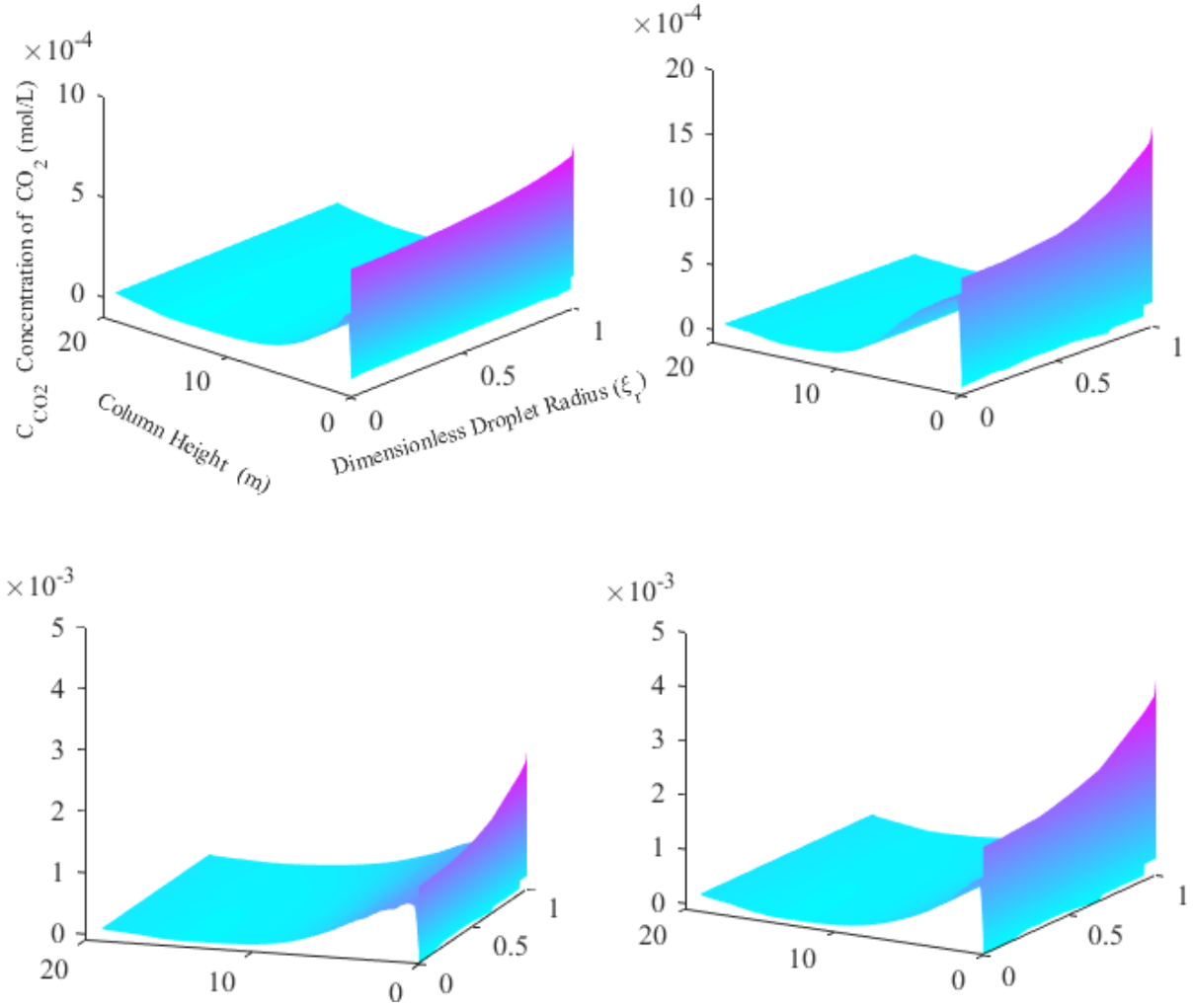

937

938 Figure S12: Case 2: CO_2 concentration profiles as function of position for $c_N = 10^7$
939 droplets/cm^3 (a) Flue gas 1, (b) Flue gas 2, (c) Flue gas 3 (d) Flue gas 4

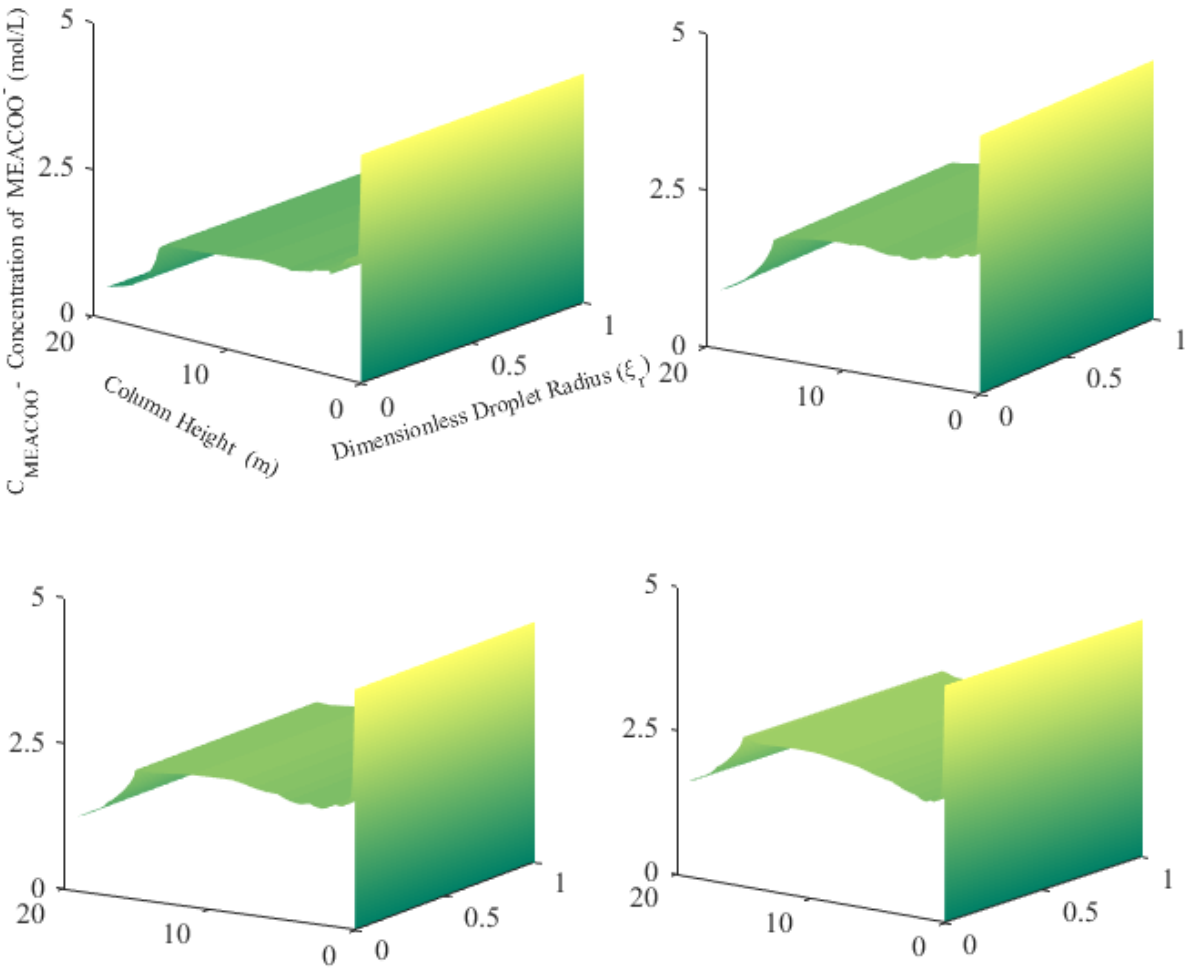

Figure S13: Case 2: Carbamate concentration profiles as function of position for c_N= 10^7 droplets/cm^3 (a) Flue gas 1, (b) Flue gas 2, (c) Flue gas 3 (d) Flue gas 4.

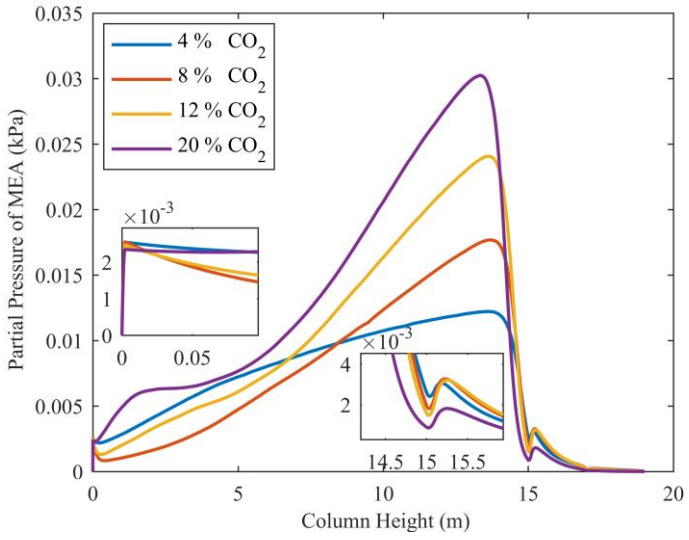

Figure S14: Case 2: Gas phase MEA partial pressure profiles for C_N= 10^7 droplets/cm^3

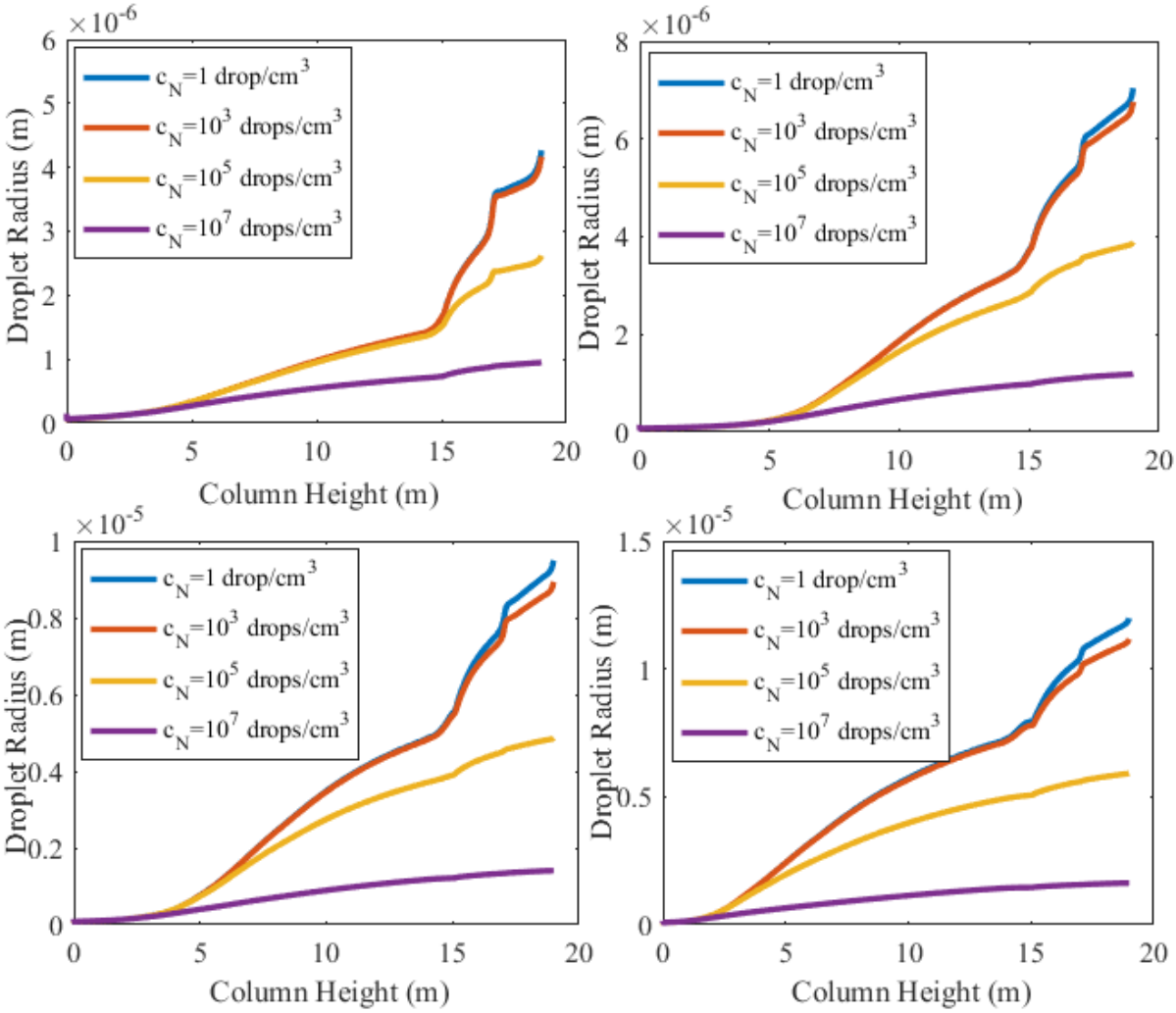

952

953 Figure S15: Case 2: Growth of aerosol droplets for all number concentrations (a) Flue
954 gas 1, (b) Flue gas 2, (c) Flue gas 3 (d) Flue gas 4.

955

956

957

958

959